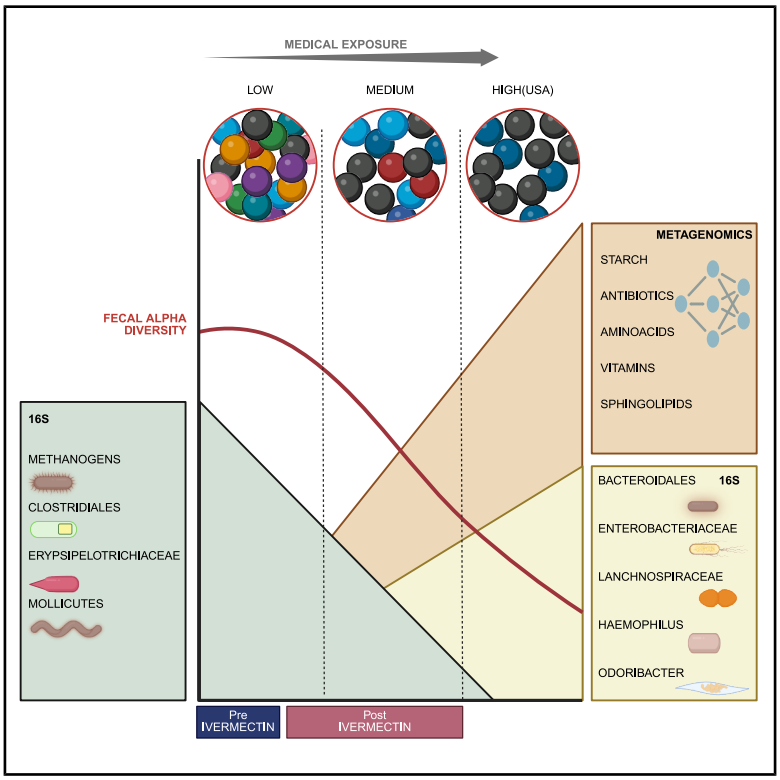
Cell Reports

Resource

Rapid microbiome restructuring associated with medical exposure in remote Amazonian Indigenous communities

Graphical abstract



Highlights

- Repeated medical exposure is associated with rapid microbiome restructuring
- Gut microbial diversity declines with repeated exposure especially in children
- Microbial taxa, networks, and gene functions shift with exposure
- Microbiome changes precede major lifestyle and dietary transition

Authors

Haipeng Sun, Oscar Noya-Alarcon, Jincheng Wang, ..., Daniela Vargas Robles, Monica Contreras, Maria G. Dominguez-Bello

Correspondence

mg.dominguez-bello@rutgers.edu

In brief

Sun et al. investigate microbiome changes across Amazonian Indigenous communities undergoing early medical exposure. They show rapid, site-specific restructuring, reduced diversity, and shifts in microbial networks and functions toward urban-associated profiles, with children exhibiting greater sensitivity to these changes.

Sun et al., 2026, Cell Reports *45*, 117343
May 26, 2026 © 2026 The Authors. Published by Elsevier Inc.
https://doi.org/10.1016/j.celrep.2026.117343

CellPress

Cell Reports

CellPress
OPEN ACCESS

Resource

Rapid microbiome restructuring associated with medical exposure in remote Amazonian Indigenous communities

Haipeng Sun,[1] Oscar Noya-Alarcon,[2] Jincheng Wang,[1] Scott G. Daniel,[3] Kyle Bittinger,[3] Wessam Mohamed,[1] Pauline D. Scanlan,[4,5] Charvi Shah,[6] Tanima Kundu,[6] Martin J. Blaser,[6] Noel T. Mueller,[7,8] Orlana Lander,[9] Mariapia Bevilaqua,[10] Daniela Vargas Robles,[11] Monica Contreras,[11] and Maria G. Dominguez-Bello[1,12,13,14,*]

[1]Department of Biochemistry & Microbiology, Rutgers University–New Brunswick, New Jersey, NJ 08901, USA
[2]Amazon Center for Research and Control of Tropical Diseases-CAICET, Puerto Ayacucho, Amazonas State, Venezuela
[3]Division of Gastroenterology, Hepatology and Nutrition, The Children's Hospital of Philadelphia, Philadelphia, PA 19104, USA
[4]School of Microbiology, University College Cork, Cork T12 YN60, Ireland
[5]APC Microbiome Ireland, University College Cork, Cork T12 YN60, Ireland
[6]Center for Advanced Biotechnology and Medicine, Rutgers University–New Brunswick, New Brunswick, NJ 08854, USA
[7]Department of Epidemiology, University of Colorado School of Medicine, Denver, CO 80045, USA
[8]Department of Pediatrics, University of Colorado School of Medicine, Aurora, CO 80045, USA
[9]Institute of Tropical Medicine, Central University of Venezuela, Caracas 1083, Venezuela
[10]Venezuelan Association for the Conservation of Natural Areas, Caracas 1050, Venezuela
[11]Venezuelan Institute of Scientific Research, Caracas 1204, Venezuela
[12]Humans and the Microbiome Program, Canadian Institute for Advanced Research, Toronto, ON, Canada
[13]Department of Anthropology, Rutgers University–New Brunswick, New Jersey, NJ 08901, USA
[14]Lead contact
*Correspondence: mg.dominguez-bello@rutgers.edu
https://doi.org/10.1016/j.celrep.2026.117343

SUMMARY

Many factors contribute to reduced microbial diversity associated with Westernization, complicating efforts to identify early drivers of microbiome change. Here, we examine microbiome variation during the introduction of a sustained medical program into previously low-exposure remote Indigenous villages. We analyze fecal samples and body-site swabs from 335 Amerindians across multiple villages before and during repeated program visits, prior to major dietary or lifestyle transitions. Low-exposure villages show higher baseline gut microbiota diversity than the medium-exposure village, and microbiota diversity declines over time in association with repeated exposure, particularly in children. Changes include loss of specific gut taxa, reduced bacterial network connectivity, and shifts in functional gene profiles toward those reported in urban populations. Oral microbiota diversity decreases, while skin and nasal diversity show modest changes. These findings indicate that repeated exposure to basic medical interventions coincides with rapid microbiome restructuring during early stages of ecological transition.

INTRODUCTION

Over 45 Indigenous nations live in Venezuela, many occupying the remote, sparsely populated jungles of the southern states of Amazonas and Bolívar.[1] Jungle villagers use their ancestral knowledge and technology to live in subsistence economies that rely on fishing, hunting, gathering, and gardening; they cultivate yucca, plantain, bananas, and pineapple. They harness natural resources for sustenance, craft tools and canoes, and build houses out of natural materials. Because of their remoteness, they are only reachable by air or river. The more-accessible villages, including those having a landing strip, are increasingly visited by medical doctors, scientists, explorers, and photographers. These more-accessible villages often have a medical post and a small school, and some residents may speak Spanish or Portuguese. In less-accessible villages, traditional lifestyles have remained largely unchanged.[1]

Onchocerciasis (river blindness) is a disease of the skin and the eye caused by *Onchocerca volvulus*, a parasitic worm transmitted by *Simulium* species (black flies) that breed in fast-flowing rivers.[2] The disease is endemic in 31 countries in sub-Saharan Africa, three countries in Latin America, and in Yemen.[3] Alongside other neglected tropical diseases (like schistosomiasis, helminthiasis, leishmaniasis, trypanosomiasis, and trachoma), it poses a significant health burden in parts of the Americas and Africa.[2] The Venezuela-Brazil border is an endemic region for *O. volvulus* and is one of the few remaining foci of this disease in the Americas.[4–6] While nodulectomy and vector control have been implemented in the past, the current intervention strategy is based on the mass drug administration of ivermectin, a

This is an open access article under the CC BY-NC-ND license (http://creativecommons.org/licenses/by-nc-nd/4.0/).

common anthelmintic also effective against some intestinal pathogenic and commensal protozoa.[7] In Africa, annual community-directed treatment with ivermectin is the main intervention in most areas except in a few foci where semi-annual treatment is implemented.[8,9] In the Americas, semi-annual ivermectin treatment with a minimum coverage of 85% is the main intervention[4]; recently, quarterly treatment has been implemented in some foci.[10]

Programs for controlling malaria, tuberculosis, and neglected tropical diseases, such as onchocerciasis, have been notably effective in non-urban regions of the world.[11,12] Specifically, the Carter Center's Onchocerciasis Elimination Program for the Americas (OEPA) has successfully led to the elimination of onchocerciasis in Colombia, Ecuador, Mexico, and Guatemala between 2013 and 2016, and efforts continue in Venezuela.[9–11,13] The program began to focus on communities from the border between Venezuela and Brazil in Bolívar state, reaching most airplane-accessible villages first in 2014.[4,5] By May and October 2015, the program extended its efforts to more-remote villages using helicopters in a region that is home to Indigenous Yek'wana and Yanomami-Sanema peoples.[4] OEPA's quarterly medical visits provide ivermectin treatments for everyone over the age of 4 years and offer other medical services as needed.[3,4] Since 1995, Yek'wana communities in the Caura River basin—and to a lesser extent Yanomami-Sanema communities—have had intermittent exposure to Western medicine,[1] but now the OEPA program reaches even remote populations quarterly (at least until the beginning of 2025), introducing them to regular medical treatments and likely fostering other influences associated with transculturation.

Urban lifestyle practices, characterized by strong antimicrobial measures, disrupt the transmission and colonization of human-coevolved microbes within the microbiota.[14–16] This interference affects developmental programming,[17–20] subsequently influencing host gene expression and contributing to immune,[19,21–23] metabolic,[16,18,24] and neurodevelopmental diseases.[25–28] While industrialization has led to improved control of many infectious diseases, it is strongly associated with reduced gut microbiota diversity,[14–16,29–32] increased antimicrobial resistance and horizontal gene transfer,[15,16,33–36] and heightened risks of chronic immune-metabolic diseases.[37–39]

The initiation of the OEPA program in Bolívar state, targeting remote Indigenous communities along the upper Caura River, provides a unique opportunity to investigate microbiome changes associated with early stages of medical exposure within broader processes linked to urbanization.

We hypothesized that rapid changes in the human microbiome coincide with increasing number of medical visits, with more pronounced changes in the developing microbiomes of children. To test this hypothesis, we conducted a longitudinal analysis of the microbiota from the most remote Amerindian villagers as they received OEPA medical visits. This analysis included comparisons between the microbiotas of children and adults from remote and more-accessible communities deep in the jungle.

Amerindian Yek'wana and Yanomami-Sanema villages are scattered in a region of 45,000 km^2 in the southern Bolívar state of Venezuela (Figure 1). We studied seven of the small remote villages as they were integrated into the OEPA medical program (before the program and the first two visits), as well as one village in which onchocerciasis is not endemic, with longer-term exposure to Western visitors and medicine. The Venezuelan research team has a long-standing history of mutual respect and collaboration with the communities involved in this study, with community members actively supporting the fieldwork by organizing logistics and serving as guides and interpreters.

Each village was categorized based on its urban exposure using previously established metrics[40] (Table S1); village exposure level accounts for the historical exposure to non-Indigenous, urban visitors and to medicines. The medium-exposure village is larger than the low-exposure villages (Figure 1; Table S2); it has a landing strip and has hosted missionaries, medical doctors, anthropologists, photographers, and other visitors since the 1970s.[1] The village also has a small school, four certified health workers who speak Spanish, and a medical post that receives intermittent supplies of antibiotics, antiparasitic drugs, analgesics, and vaccines. Although this village is not part of the onchocerciasis-endemic area and is excluded from the OEPA program, it serves as the program's operational center in the region. Quarterly, an airplane lands there with supplies that are then transported by helicopter to the seven endemic remote villages, in a logistical operation coordinated by Dr. Noya-Alarcon. The program provides ivermectin treatment to all persons in endemic areas older than 4 years of age, in the dose recommended by the WHO (150 μg/kg body weight[5]). With these medical visits, all villages receive medical attention and basic medication, most commonly vaccines, amoxicillin, analgesics, antifungals, non-steroidal anti-inflammatory drugs, and vitamins. This study design allows separation of long-term urban exposure from short-term exposure associated with OEPA program visits.

RESULTS

Sampling visits were conducted in October 2015 and February 2016 (Table S2), during the dry season; thus food variations are relatively limited. Across both visits, a total of 1,506 samples were obtained from 335 participants (200 children and 75 adults; Tables S3 and S4), including 97 samples collected from the same individuals at both time points. Fecal specimens and oral, nasal, and skin swabs were processed for DNA extraction; fecal samples were analyzed by shotgun metagenomic sequencing and all samples by *16S rRNA* gene amplicon sequencing.

Fecal microbiome

This study examines microbiome variation along two partially independent axes: (1) differences across villages with distinct long-term levels of urban exposure (low vs. medium exposure) and (2) longitudinal changes within low-exposure villages associated with repeated OEPA program visits, which introduce medical teams and medicines.

Shotgun metagenomic fecal analyses (Table S5) revealed pronounced differences in the fecal β-diversity of Amerindian villagers according to the level of urban exposure during the first visit in 2015. Here, "urban exposure" reflects historical and infrastructural contact with non-Indigenous visitors, including the

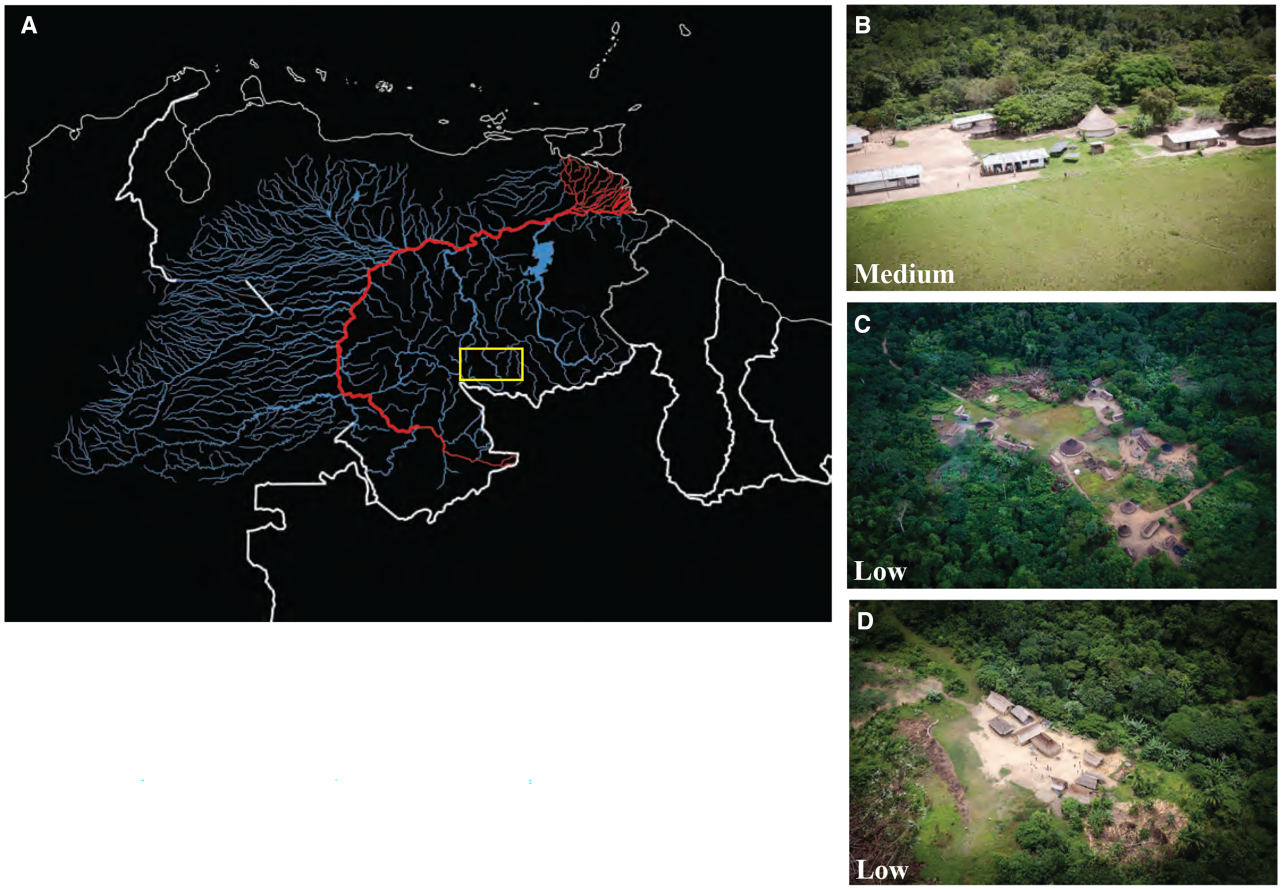


Figure 1. Geographic location and exposure context of study villages

(A) Map of the Orinoco River Basin showing the locations of the study villages. The main channel of the Orinoco River is shown in red and its tributaries in blue; the study region is highlighted in yellow.

(B) Aerial view of the medium-urban-exposure Yek'wana village of Kanarakuni.

(C) Aerial view of the low-urban-exposure Yek'wana village of Fiyakwanha.

(D) Aerial view of the low-urban-exposure Yanomami-Sanema village of Shianana.

White text in (B–D) indicates relative levels of exposure to visitors, urban practices, medical care, and medicines (see urban exposure score in Table S1).

presence of an airstrip, school, and medical post, rather than participation in the OEPA program. These differences were no longer significant at the second visit in 2016 (Figures 2A and 2B; Table S5), consistent with rapid microbiome restructuring over time within low-exposure villages following repeated program visits. Compared with US subjects, the fecal microbiota of Amerindians had not yet converged toward the typical Western configuration (Figure 2C), consistent with an ongoing transitional state. Urban exposure-related alterations were further supported by network analyses, which showed lower connectivity and higher node degree in US subjects relative to Amerindian villagers (Figure S1).

Taxa decreasing with exposure

Although shotgun metagenomic analyses revealed no significant differences in α-diversity between exposure levels (Figure S2; Table S6), taxonomic composition shifted markedly along the urban exposure gradient. Bacterial taxa characteristic of low-exposure, traditional microbiomes were consistently diminished along the urban exposure gradient, most notably members of the genera *Prevotella* (Bacteroidota) and *Treponema* (Spirochaetota) and families Ruminococcaceae and Lachnospiraceae (Bacillota), (Figures 2D–2F; Table S7), which include hallmark fiber-degrading and short-chain fatty acid (SCFA)-producer bacteria. Medium-exposure children sampled in 2015 exhibited reduced relative abundance of *Anaerovibrio*, *Roseburia*, *Ruminococcus*, *Anaerostipes*, and multiple *Prevotella* species, with additional reductions in 2016 that included *Collinsella* and *Treponema* (Figures 2D and 2E; Table S7). Compared to Indigenous participants, the US reference samples showed broader depletion across multiple lineages, including marked losses of *Prevotella*, *Brachyspira*, *Succinivibrio*, *Treponema peruenese*, and *Mycoplasma* (Figure 2F; Table S7). Across the wide extremes of exposure—from low through medium to US reference populations—a subset of fecal bacterial taxa showed a consistent directional decline with increasing urban exposure, including

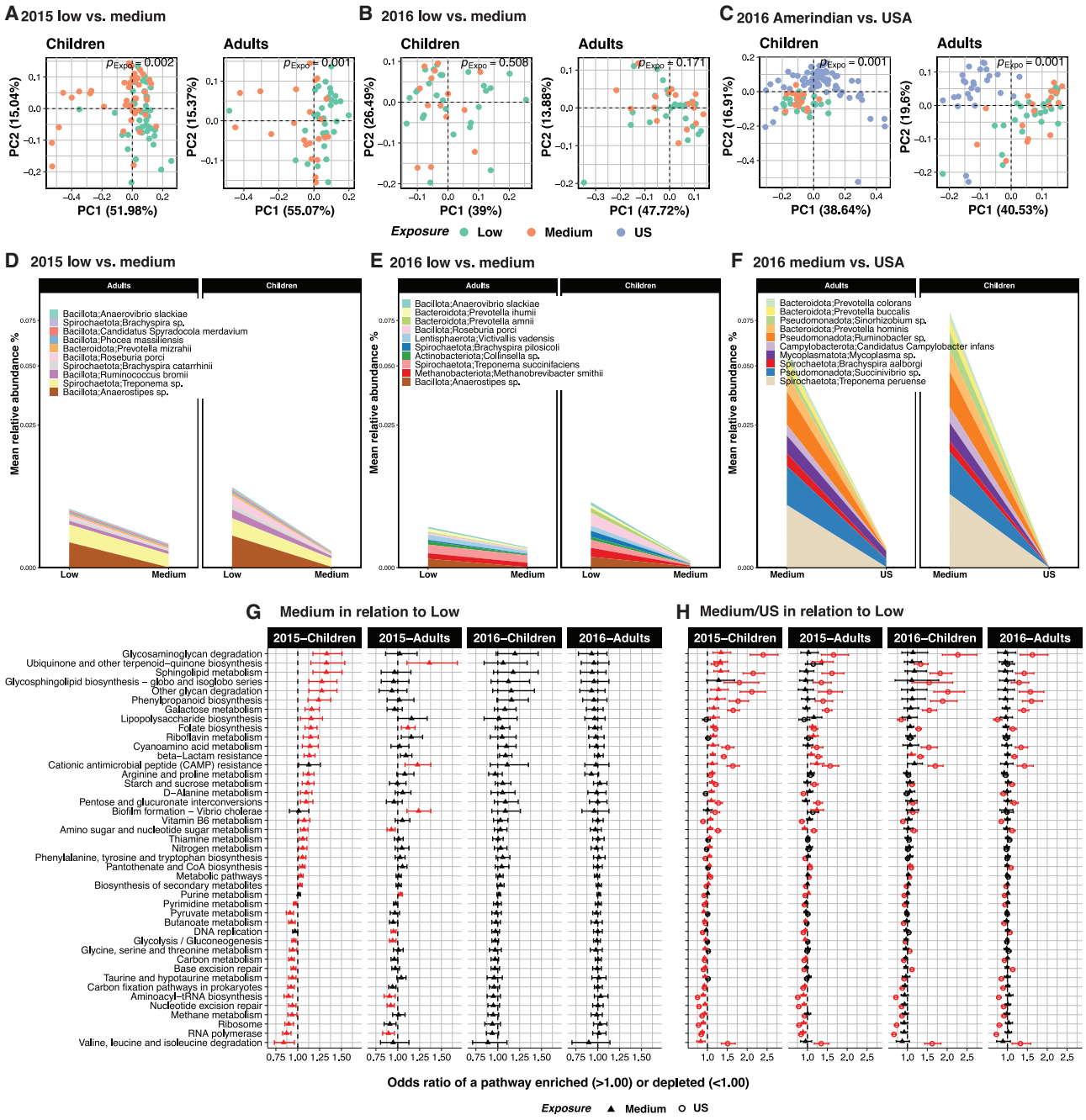


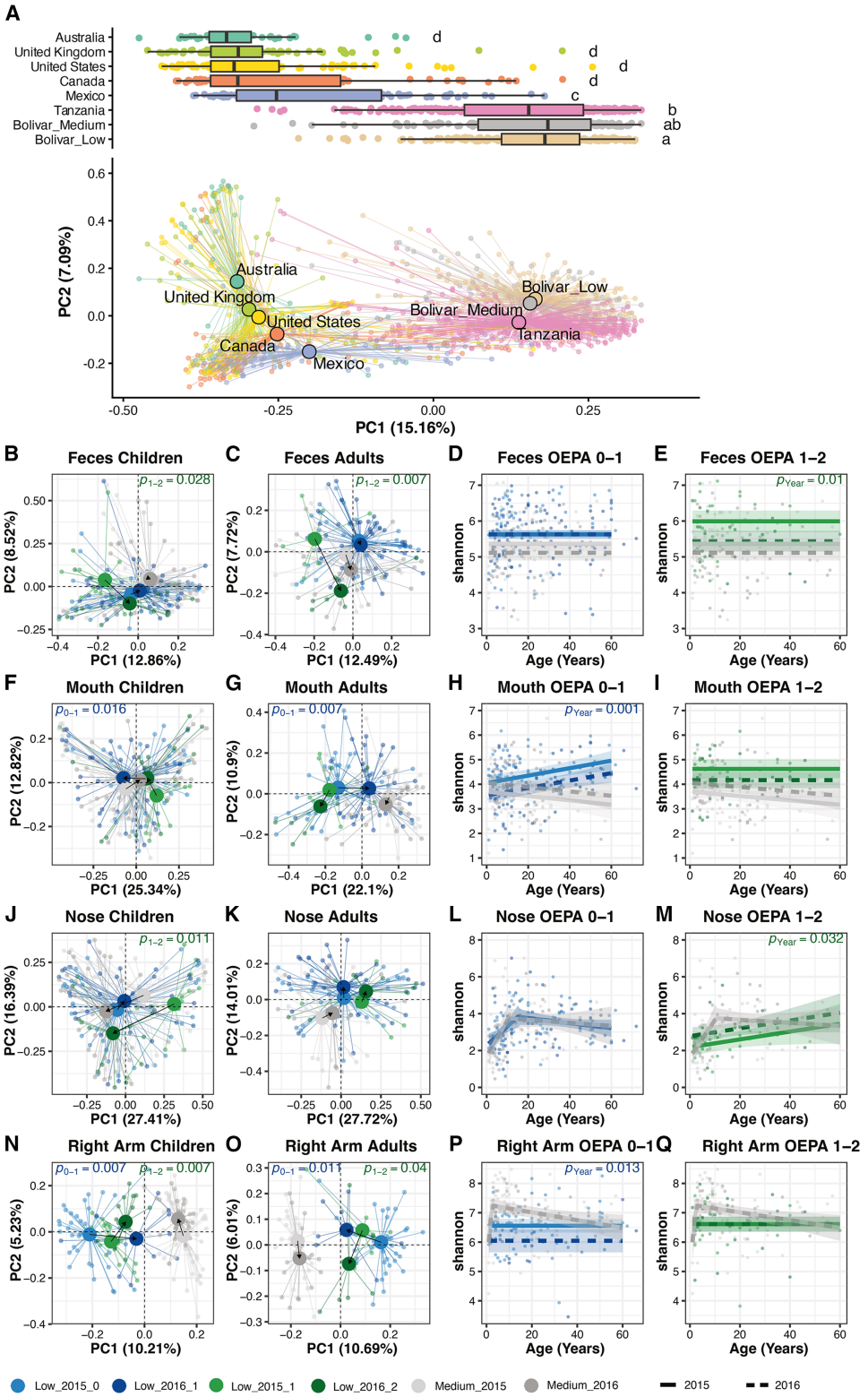
Figure 2. Metagenomic-based fecal microbiome and functional profiles across the urban exposure gradient

(A–C) Shotgun metagenomic Bray-Curtis β-diversity distances in children and adults: (A) comparisons between villages in 2015, (B) comparisons between villages in 2016, and (C) comparisons between Amerindian and US reference subjects in 2016.

(D–F) The 10 most abundant fecal bacterial taxa with decreased relative abundance in children across exposure contrasts: (D) medium- versus low-urban-exposure villages in 2015, (E) medium- versus low-urban-exposure villages in 2016, and (F) medium-urban-exposure villages versus US reference subjects in 2016.

(G and H) Odds ratios (ORs) of metagenomic functional gene pathways relative to low-urban-exposure villages are shown for (G) medium-urban-exposure villagers and (H) US reference subjects compared with medium-urban-exposure villagers. Red brackets denote pathways with statistically significant differences (false discovery rate [FDR]-corrected $p < 0.05$). ORs >1 or <1 indicate relative enrichment or reduction, respectively.

CellPress
OPEN ACCESS



(legend on next page)

multiple Spirochaetota (*Brachyspira* spp. and *Treponema* spp.); anaerobic and fermentative lineages such as *Anaerovibrio slackiae*, *Roseburia porci*, *Enterocloster citroniae*, and *Oribacterium* sp.; as well as several enteric or mucosa-associated bacteria, including *Helicobacter pylori* and *Shigella sonnei* (Table S7).

Consistent with these findings, *16S rRNA* gene analyses confirmed significant β-diversity differences across urban exposure categories (Figure 3). The fecal microbiota structure of low- and medium-exposure villages in this study were most similar to that of the Hadza people in Tanzania, clustering apart from urban populations in Mexico, North America, and the United Kingdom (Figure 3A), forming a shared cluster of traditional lifestyle populations. Within this cluster, fecal β-diversity differed significantly between Tanzania and low-urban-exposure Bolívar villages (Figure 3A top).

Direct comparisons of β-diversity across OEPA visit numbers within low-urban-exposure villages showed significant compositional differences (Figures 3B and 3C; Tables S8 and S9). These shifts were accompanied by a reduction in fecal α-diversity between visits 1 and 2 ($p = 0.01$; Figures 3D and 3E; Table S10), alongside declines in taxa spanning Bacillota (Ruminococcaceae and Erysipelotrichaceae), Actinobacteria (*Collinsella*), Mycoplasmatota (Mollicutes RF39), and Methanobacteriota (*Methanobrevibacter*) (Figure S3).

Taxa increasing with exposure

Conversely, Table S7 identifies a complementary set of fecal taxa whose relative abundance increases with increasing urban exposure (i.e., taxa enriched in medium-exposure villages and/or further enriched in US reference samples). These "urban-enriched" lineages were dominated by taxa commonly observed in gut configurations in people in more-industrialized settings,[14,30,32,35,41] including multiple Bacteroidota (e.g., *Alistipes* spp., *Bacteroides* spp., *Parabacteroides distasonis*, and *Phocaeicola* spp.), Verrucomicrobia (*Akkermansia muciniphila*), and select additional taxa showing consistent directional enrichment across the low→medium→US gradient (Table S7).

Intestinal parasites

Finally, there was a high prevalence of intestinal parasites across exposure levels. *Blastocystis* colonization patterns varied markedly with long-term urban exposure and geography (Figure S4). Multi-subtype colonization (triple or quadruple species subtypes) predominantly among villagers with very low and low urban exposure, whereas medium-exposure individuals and reference populations from Caracas showed fewer mixed infections. In contrast, single-subtype colonization dominated in highly urbanized reference populations from Ireland and the United States, consistent with reduced intestinal microbial and protistan diversity in industrialized settings (Figure S5). The burden of other parasites (Table S11) was broadly comparable across villages, although *Trichuris trichiura* was significantly reduced in medium-exposure villagers in 2016 ($p = 0.025$). *Entamoeba coli* cysts and *Chilomastix mesnili* cysts also showed differential prevalence ($p = 0.049$ and $p < 0.001$, respectively), suggesting partial shifts in enteric parasite ecology associated with increasing medical exposure and sanitation.

Fecal functional differences by urban exposure

Shotgun metagenomic analyses of fecal gene content revealed pronounced restructuring of microbial metabolic potential along the urbanization gradient, consistent across comparisons among Amerindian villages with differing exposure levels (Figure 2G; Table S12). When data from all Amerindian groups were pooled and compared with those from the US population, the same functional pathways showed even greater divergence, underscoring the profound impact of urbanization on microbial metabolic functions (Figure 2H; Table S13).

Among the 43 pathways that changed with exposure, 27 were increased with urban exposure, including starch and sucrose metabolism, galactose metabolism, pentose and glucuronate interconversions, amino sugar and nucleotide sugar metabolism, and glycosaminoglycan degradation—reflecting shifts in carbohydrate utilization pathways. Genes associated with antimicrobial resistance, including beta-lactam and cationic antimicrobial peptide resistance, were also enriched in the medium-exposure and US subjects (Figures 2G and 2H).

The remaining 16 pathways that declined with increasing urban exposure were primarily associated with core biosynthetic, energy, and repair processes (Figure 2G; Table S12). Reductions in glycolysis/gluconeogenesis, pyruvate and carbon metabolism, and amino acid (valine, leucine, and isoleucine) degradation genes suggest altered central carbon flux and increased reliance on simpler substrates. Consistent with these functional patterns, fecal acetate concentrations were lower in adults from the medium-exposure village than in those from the low-exposure village (Figure S6). Decreases in genes involved in methane and taurine metabolism were also observed, and qPCR analyses

Figure 3. *16S rRNA*-based microbiota diversity across body sites and visits

(A) Fecal Bray-Curtis β-diversity comparing Venezuelan Indigenous populations with global reference populations (American Gut Project and Hadza-hunter-gatherer cohort, Tanzania). Points are colored by population. Boxplots show the distribution of samples of each population along principal coordinate 1 (PC1). Letters indicate statistically significant differences between populations (Kruskal-Wallis pairwise comparisons).

(B, F, J, and N) Bray-Curtis β-diversity for children (<18 years) from feces, oral cavity, nasal cavity, and skin, respectively. *p* values indicate significant PERMANOVA tests across OEPA visit numbers within low-urban-exposure villages.

(C, G, K, and O) Bray-Curtis β-diversity for adults (≥18 years) from feces, oral cavity, nasal cavity, and skin, respectively. Large symbols indicate visit group centroids; small symbols indicate individual samples. *p* values indicate significant PERMANOVA tests across OEPA visit numbers within low-urban-exposure villages. Blue shades denote low-exposure villages sampled at visit 0 or visit 1 (2015); green shades denote visit 1 or visit 2 (2016); gray denotes the medium-urban-exposure village (not enrolled in the OEPA program).

(D, H, L, and P) Shannon α-diversity comparisons between OEPA visit 0 and visit 1 (solid blue, visit 0; segmented blue, visit 1).

(E, I, M, and Q) Shannon α-diversity comparisons between OEPA visit 1 and visit 2 (solid green, visit 1; segmented green, visit 2). Gray symbols and lines represent the medium-urban-exposure village, shown for reference only.

confirmed lower methanogen abundance in children from medium- compared with low-exposure villages (Figure S7).

Multiple body-site microbiota diversity

Consistent with cumulative medical exposure across visits, fecal and oral β-diversity differences were significant between visits in low-exposure villagers (PERMANOVA, p adj = 0.002; Table S8). *16S rRNA* gene analyses confirmed shotgun findings (Figure 3), except for a significantly higher α-diversity in low-exposure villagers (Table S10). Both Amerindian groups exhibited greater diversity than US subjects, with the highest richness observed among low-exposure children (Figure S2; Table S6).

For other body sites, oral microbiotas showed significant β-diversity separation across exposure levels in both children and adults (Figures 3F and 3G; Table S9), as did nasal microbiotas in children (Figure 3J; Table S9) and skin communities (Figures 3N and 3O; Table S9). Increasing exposure across visits generally reduced α-diversity, except in the nose where it increased after two visits (Figure 3M; Table S10). In medium-exposure villages, α-diversity did not show a significant difference except in the oral microbiota (Table S10).

The oral microbiota showed a significant decline in α-diversity after the first OEPA visit ($p < 0.001$; Figure 3H; Table S10), with a consistent, but nonsignificant, downward trend after the second visit (Figure 3I; Table S10). Vanishing oral taxa spanned multiple phyla, including *Fusobacterium* (Fusobacteriota), *Alloprevotella* (Bacteroidota), and several Proteobacteria (*Aggregatibacter*, *Campylobacter*, and *Moraxella*), indicating broad depletion across anaerobic and facultative lineages (Figure S8).

The nasal microbiota exhibited the opposite trend, with α-diversity increasing significantly between the first and second visits ($p = 0.03$; Figure 3L; Table S10). Compositionally, nasal communities showed reductions in Actinobacteria, including *Nesterenkonia*, *Ornithinicoccus*, *Dietzia*, *Aeromicrobium*, and *Brevibacterium* (Figure S9).

The skin microbiota α-diversity tended to decrease after the first OEPA visit ($p = 0.013$; Figure 3P; Table S10), with taxonomic losses on the right arm including Actinobacteriota (*Nesterenkonia*, *Glutamicibacter*, and *Aeromicrobium*), Bacillota (*Exiguobacterium* and *Pediococcus*), and Bacteroidota (*Porphyromonas*) (Figure S10).

DISCUSSION

This study leverages a rare longitudinal dataset from remote Amazonian Indigenous communities to examine how the human microbiome shifts during the earliest stages of contact with external institutions, prior to major dietary or lifestyle urbanization. By sampling communities before and after their integration into a large-scale public health program, and by contrasting low- and medium-exposure villages, we capture microbiome restructuring that occurs alongside initial, limited interactions with outsiders rather than as a consequence of broader urbanization processes. Sampling occurred between early October 2015 and mid-February 2016, corresponding to the dry season, when seasonal variation in food availability is likely reduced in this tropical context; plant foods are largely derived from household gardens, and many fruits and animal foods are available year-round. To our knowledge, no additional organized groups visited these remote communities between sampling points, and interactions with visitors were brief and centered on medical activities, without food distribution.

Interpretation of these findings requires consideration of non-medical exposures associated with repeated program visits. Although OEPA visits involved the arrival of external personnel, interactions were brief, episodic, and centered on medical screening and treatment, without prolonged social engagement or environmental disturbance. No non-local food sources were brought in or distributed during medical campaigns, and subsistence practices based on hunting, fishing, gathering, and household gardening remained unchanged. Sampling occurred between early October 2015 and mid-February 2016, during the dry season, yet, seasonal dietary variation cannot be excluded as contributor to the observed gut microbiome changes. To our knowledge, no additional organized groups visited the remote villages between sampling points. While unmeasured factors such as transient infections or short-term behavioral changes cannot be fully excluded, the consistency of microbiome shifts across visits, body sites, and exposure gradients suggests that the observed restructuring reflects cumulative external exposure associated with early program contact rather than abrupt changes in diet, climate, or village social structure.

Although multiple factors may contribute to temporal microbiome change—including short-term dietary fluctuations, interannual climatic variation, concurrent medical encounters, and unmeasured infections—the coherence of observed shifts across time, body sites, and exposure gradients is consistent with the interpretation that microbiome "Westernization" can begin rapidly, even in the absence of overt lifestyle change. This natural experiment, therefore, provides a unique and early view of microbiome transitions that are typically obscured by many confounded elements of industrialization.[14–16,29–32]

Across body sites, microbiome composition and diversity consistently differed by exposure level and across visits, with particularly pronounced effects observed in children. In the gut, the reduced lineages—*Prevotella*, *Treponema*, *Methanobrevibacter*, *Ruminococcaceae*, and *Lachnospiraceae*—form part of the microbial guilds that sustain fermentation, hydrogen turnover, and SCFA production.[42–49] These lineages have been repeatedly associated with high-fiber diets and complex carbohydrate fermentation in non-industrialized populations,[14–16,29–32] and their loss in this context mirrors patterns reported across diverse global comparisons of traditional and urbanized populations.

Functional profiling based on metagenomic gene content revealed coordinated shifts in metabolic potential associated with exposure, including enrichment of pathways related to simple carbohydrate utilization and antimicrobial resistance, alongside reductions in pathways linked to core biosynthetic and energy metabolism. Although only acetate concentrations differed significantly between exposure groups, the convergence of taxonomic, network, functional gene, and metabolite patterns is consistent with a partial erosion of fermentative capacity.[15,16,29] These findings echo prior work demonstrating that loss of fiber-degrading taxa precedes more extensive

functional erosion in urbanized microbiomes,[14–16,30–32] while also underscoring that functional redundancy may buffer some metabolic outputs during early stages of transition.

Children exhibited the most pronounced microbiome changes across visits, consistent with heightened sensitivity of the developing microbiome to ecological perturbation.[18,19,29,50–52] Early-life microbial communities play a critical role in immune, metabolic, and neurodevelopmental programming,[18,19,29,37–39,50–52] and even modest disruptions during this period may have disproportionate downstream consequences. While our study was not designed to assess clinical outcomes, the observed patterns raise important questions about how repeated medical visits during early childhood may intersect with long-term health trajectories in populations undergoing societal transition.

Beyond the gut, oral, nasal, and skin microbiotas also showed exposure-associated restructuring, although with site-specific patterns. Oral microbiota diversity declined with exposure, accompanied by loss of anaerobic and several genera that include known oral pathobionts, suggesting that medical exposure may simultaneously reduce microbial diversity and alter pathogen-associated niches.[21–23,53,54] Notably, some taxa that declined in the oral microbiome, including *Campylobacter* and *Aggregatibacter*, are commonly associated with oral pathobionts, indicating that not all observed microbial losses necessarily represent adverse ecological change. In contrast, nasal microbiota diversity increased across visits, while skin communities showed declining diversity and loss of multiple Actinobacteriota and Bacillota taxa. Together, these findings highlight that microbiome responses to early medical exposure are not uniform across body sites, but instead reflect distinct ecological dynamics shaped by local selective pressures.

The inclusion of a medium-exposure village not participating in the onchocerciasis elimination program is critical for interpreting these patterns. This village serves as a reference for sustained medical and urban exposure independent of the OEPA intervention. Comparisons across villages, therefore, allow partial separation of short-term exposure associated with program visits from longer-term exposure linked to infrastructure and sustained contact, strengthening inference while remaining within the constraints of an observational design.

From a broader perspective, these findings contribute to an emerging understanding of microbiome "Westernization" as a process that begins early and progresses incrementally.[14–16,29–32] While the benefits of infectious disease control are indisputable,[2,8–11,13] our data suggest that even essential medical interventions may coincide with unintended ecological consequences for the human microbiome, particularly in populations that have historically maintained high gut microbial diversity. This underscores the importance of developing public health strategies that both preserve the lifesaving benefits of medicine and remain attentive to the long-term ecological dimensions of human-microbe relationships.

The coherence of patterns across taxonomic, network, functional gene, and metabolite analyses supports that early exposure to medical teams and medicines is closely associated with rapid microbiome restructuring. For Indigenous communities in transition, this represents a profound trade-off: access to modern medical care reduces infectious disease burden, yet it may also coincide with diminishing microbial diversity that has co-evolved with traditional lifestyles[14–16,29] and increasing risk of chronic diseases.[19,21–23,54–58] Understanding and navigating this balance is essential not only for microbiome science but also for ethical, culturally informed approaches that respect both biological and social dimensions of well-being.

Limitations of the study

This observational study offered a rare opportunity to examine microbiome restructuring associated with early medical exposure in remote Indigenous villages. Several limitations should be acknowledged. (1) The study is observational, and unmeasured factors associated with repeated medical visits and mass drug administration—including transient infection dynamics, environmental changes, or dietary fluctuations—may have contributed to the observed changes. (2) Only one medium-exposure village was included as a reference not in the OEPA program. (3) Clinical endpoints such as immune markers, growth, and inflammation could not be collected due to permit constraints.[18,19,29,37–39,50–52] (4) While microbiome profiles consistently shifted with exposure across multiple body sites, long-term recovery or resilience could not be evaluated. (5) The study lacks the longitudinal and integrative approaches needed to understand the complex interactions between medical interventions and the ecology of the human microbiome during early stages of societal transition.

RESOURCE AVAILABILITY

Lead contact

Further information and requests for resources and reagents should be directed to and will be fulfilled by the lead contact, Maria Gloria Domínguez-Bello (mg.dominguez-bello@rutgers.edu).

Materials availability

Samples from Indigenous peoples are restricted by the Venezuelan Bioethical Committee and may only be used for the approved research purposes.

Data and code availability

16S rRNA gene and metagenomic sequences have been deposited in the European Nucleotide Archive (ENA) under accession number ENA: PRJEB55648. All data are available under a CC-BY-ND 4.0 International license. This paper does not report original code.

ACKNOWLEDGMENTS

We thank the inhabitants of the Alto Caura region and the leaders and health workers of the Yek'wana villages, Rómulo Rodríguez, Yanmadi (Nelson Rojas García), and Mayde'duwa (Saúl Alango Pinto)—as well as María and Domingo from Yanomami-Sanema communities—for their assistance and interpretation during fieldwork. Their collaboration made this study possible. We thank Luna Wang for her help with editing the figures. We also acknowledge financial support from CIFAR, the C&D Fund, and the Emch Fund (to M.G.D.-B.).

AUTHOR CONTRIBUTIONS

Conceptualization, M.G.D.-B., M.C., and O.N.-A.; methodology, M.G.D.-B., M.C., J.W., H.S., S.G.D., K.B., W.M., P.D.S., C.S., T.K., M.J.B., O.L., M.B.,

and D.V.R.; analysis, M.G.D.-B., H.S., J.W., S.G.D., K.B., P.D.S., C.S., T.K., and M.J.B.; resources, O.N.-A., M.C., and M.G.D.-B.; sample processing, H.S., J.W., S.G.D., and K.B.; writing – original draft, M.G.D.-B., H.S., and J.W. Manuscript edited by all authors.

DECLARATION OF INTERESTS

The authors declare no competing interests.

STAR★METHODS

Detailed methods are provided in the online version of this paper and include the following:

- KEY RESOURCES TABLE
- EXPERIMENTAL MODEL AND STUDY PARTICIPANT DETAILS
  - Subjects and samples
- METHOD DETAILS
  - Library preparation and sequencing
  - *16S rRNA* sequencing data processing
  - Shotgun metagenomic sequencing data processing
  - Quantitative real-time PCR of methanogens
  - Fecal volatile fatty acid analysis
  - Intestinal parasites detection
- QUANTIFICATION AND STATISTICAL ANALYSIS
  - Microbiota diversity analyses
  - Gene pathways analyses
  - Differential taxa analyses
  - Co-abundance network analyses

SUPPLEMENTAL INFORMATION

Supplemental information can be found online at https://doi.org/10.1016/j.celrep.2026.117343.

Received: October 30, 2025
Revised: March 5, 2026
Accepted: April 13, 2026
Published: May 20, 2026

REFERENCES

1. Bevilacqua, M., Medina, D.A., Cárdenas, L., Rubio-Palis, Y., Moreno, J., Martínez, A., and Simplificada A.de, M. (2009). Caura M.I.d. Orientaciones para fortalecer el programa de malaria en zonas remotas con población indígena en el Caura, Venezuela. Boletin de Malariologia y Salud Ambiental XLIX *49*, 53–72.
2. WHO (2019). Onchocerciasis (river blindness). https://www.who.int/news-room/fact-sheets/detail/onchocerciasis.
3. WHO (2016). Guidelines for Stopping Mass Drug Administration and Verifying Elimination of Human Onchocerciasis: Criteria and Procedures.Geneva (World Health Organization). https://apps.who.int/iris/handle/10665/204180.
4. Noya-Alarcon, O. (2015). OEPA PNEO:FS Report, High Caura, Venezuela.Onchocerciasis Elimination Program for the Americas (OEPA).
5. Botto, C., Basañez, M.G., Escalona, M., Villamizar, N.J., Noya-Alarcón, O., Cortez, J., Vivas-Martínez, S., Coronel, P., Frontado, H., Flores, J., et al. (2016). Evidence of suppression of onchocerciasis transmission in the Venezuelan Amazonian focus. Parasit. Vectors *9*, 40. https://doi.org/10.1186/s13071-016-1313-z.
6. Botto, C., Escalona, E., Vivas-Martinez, S., Behm, V., Delgado, L., and Coronel, P. (2005). Geographical patterns of onchocerciasis in southern Venezuela: relationships between environment and infection prevalence. Parassitologia *47*, 145–150.
7. Roberts, T., Bush, S., Ellis, J., Harkness, J., and Stark, D. (2015). In Vitro Antimicrobial Susceptibility Patterns of Blastocystis. Antimicrob. Agents Chemother. *59*, 4417–4423. https://doi.org/10.1128/AAC.04832-14.
8. CDI Study Group (2010). Community-directed interventions for priority health problems in Africa: results of a multicountry study. Bull. World Health Organ. *88*, 509–518. https://doi.org/10.2471/BLT.09.069203.
9. Sauerbrey, M. (2008). The Onchocerciasis Elimination Program for the Americas (OEPA). Ann. Trop. Med. Parasitol. *102*, 25–29. https://doi.org/10.1179/136485908X337454.
10. Lovato, R., Guevara, A., Guderian, R., Proaño, R., Unnasch, T., Criollo, H., Hassan, H.K., and Mackenzie, C.D. (2014). Interruption of infection transmission in the onchocerciasis focus of Ecuador leading to the cessation of ivermectin distribution. PLoS Negl. Trop. Dis. *8*, e2821. https://doi.org/10.1371/journal.pntd.0002821.
11. Blanks, J., Richards, F., Beltrán, F., Collins, R., Alvarez, E., Zea Flores, G., Bauler, B., Cedillos, R., Heisler, M., Brandling-Bennett, D., et al. (1998). The Onchocerciasis Elimination Program for the Americas: a history of partnership. Rev Panam Salud Publica *3*, 367–374. https://doi.org/10.1590/s1020-49891998000600002.
12. World Health Organization (WHO) (2020). Ending the neglect to attain the Sustainable Development Goals: a road map for neglected tropical diseases 2021–2030 (Geneva: World Health Organization). https://www.who.int/publications/i/item/9789240010352.
13. Sauerbrey, M., Rakers, L.J., and Richards, F.O. (2018). Progress toward elimination of onchocerciasis in the Americas. Int. Health *10*, i71–i78. https://doi.org/10.1093/inthealth/ihx039.
14. Yatsunenko, T., Rey, F.E., Manary, M.J., Trehan, I., Dominguez-Bello, M.G., Contreras, M., Magris, M., Hidalgo, G., Baldassano, R.N., Anokhin, A.P., et al. (2012). Human gut microbiome viewed across age and geography. Nature *486*, 222–227. https://doi.org/10.1038/nature11053.
15. Clemente, J.C., Pehrsson, E.C., Blaser, M.J., Sandhu, K., Gao, Z., Wang, B., Magris, M., Hidalgo, G., Contreras, M., Noya-Alarcón, Ó., et al. (2015). The microbiome of uncontacted Amerindians. Sci. Adv. *1*, e1500183. https://doi.org/10.1126/sciadv.1500183.
16. Sonnenburg, J.L., and Sonnenburg, E.D. (2019). Vulnerability of the industrialized microbiota. Science *366*, eaaw9255. https://doi.org/10.1126/science.aaw9255.
17. Cox, L.M., Yamanishi, S., Sohn, J., Alekseyenko, A.V., Leung, J.M., Cho, I., Kim, S.G., Li, H., Gao, Z., Mahana, D., et al. (2014). Altering the intestinal microbiota during a critical developmental window has lasting metabolic consequences. Cell *158*, 705–721. https://doi.org/10.1016/j.cell.2014.05.052.
18. Martinez, K.A., 2nd, Devlin, J.C., Lacher, C.R., Yin, Y., Cai, Y., Wang, J., and Dominguez-Bello, M.G. (2017). Increased weight gain by C-section: Functional significance of the primordial microbiome. Sci. Adv. *3*, eaao1874. https://doi.org/10.1126/sciadv.aao1874.
19. Livanos, A.E., Greiner, T.U., Vangay, P., Pathmasiri, W., Stewart, D., McRitchie, S., Li, H., Chung, J., Sohn, J., Kim, S., et al. (2016). Antibiotic-mediated gut microbiome perturbation accelerates development of type 1 diabetes in mice. Nat. Microbiol. *1*, 16140. https://doi.org/10.1038/nmicrobiol.2016.140.
20. Zhang, X.-S., Li, J., Krautkramer, K.A., Badri, M., Battaglia, T., Borbet, T.C., Koh, H., Ng, S., Sibley, R.A., Li, Y., et al. (2018). Antibiotic-induced acceleration of type 1 diabetes alters maturation of innate intestinal immunity. eLife *7*, e37816. https://doi.org/10.7554/elife.37816.
21. Cait, A., Hughes, M.R., Antignano, F., Cait, J., Dimitriu, P.A., Maas, K.R., Reynolds, L.A., Hacker, L., Mohr, J., Finlay, B.B., et al. (2018). Microbiome-driven allergic lung inflammation is ameliorated by short-chain fatty acids. Mucosal Immunol. *11*, 785–795. https://doi.org/10.1038/mi.2017.75.
22. Kristensen, K., and Henriksen, L. (2016). Cesarean section and disease associated with immune function. J. Allergy Clin. Immunol. *137*, 587–590. https://doi.org/10.1016/j.jaci.2015.07.040.

23. Schroeder, B.O., and Bäckhed, F. (2016). Signals from the gut microbiota to distant organs in physiology and disease. Nat. Med. *22*, 1079–1089. https://doi.org/10.1038/nm.4185.

24. Cox, L.M., and Blaser, M.J. (2015). Antibiotics in early life and obesity. Nat. Rev. Endocrinol. *11*, 182–190. https://doi.org/10.1038/nrendo.2014.210.

25. Hsiao, E.Y., McBride, S.W., Hsien, S., Sharon, G., Hyde, E.R., McCue, T., Codelli, J.A., Chow, J., Reisman, S.E., Petrosino, J.F., et al. (2013). Microbiota modulate behavioral and physiological abnormalities associated with neurodevelopmental disorders. Cell *155*, 1451–1463. https://doi.org/10.1016/j.cell.2013.11.024.

26. Sharon, G., Cruz, N.J., Kang, D.W., Gandal, M.J., Wang, B., Kim, Y.M., Zink, E.M., Casey, C.P., Taylor, B.C., Lane, C.J., et al. (2019). Human Gut Microbiota from Autism Spectrum Disorder Promote Behavioral Symptoms in Mice. Cell *177*, 1600–1618.e17. https://doi.org/10.1016/j.cell.2019.05.004.

27. Vuong, H.E., and Hsiao, E.Y. (2017). Emerging Roles for the Gut Microbiome in Autism Spectrum Disorder. Biol. Psychiatry *81*, 411–423. https://doi.org/10.1016/j.biopsych.2016.08.024.

28. Cryan, J.F., and Dinan, T.G. (2012). Mind-altering microorganisms: the impact of the gut microbiota on brain and behaviour. Nat. Rev. Neurosci. *13*, 701–712. https://doi.org/10.1038/nrn3346.

29. Blaser, M.J., and Dominguez-Bello, M.G. (2025). The Invisible Extinction. Annu. Rev. Microbiol. *79*, 311–334. https://doi.org/10.1146/annurev-micro-051024-092416.

30. De Filippo, C., Cavalieri, D., Di Paola, M., Ramazzotti, M., Poullet, J.B., Massart, S., Collini, S., Pieraccini, G., and Lionetti, P. (2010). Impact of diet in shaping gut microbiota revealed by a comparative study in children from Europe and rural Africa. Proc. Natl. Acad. Sci. USA *107*, 14691–14696. https://doi.org/10.1073/pnas.1005963107.

31. Smits, S.A., Leach, J., Sonnenburg, E.D., Gonzalez, C.G., Lichtman, J.S., Reid, G., Knight, R., Manjurano, A., Changalucha, J., Elias, J.E., et al. (2017). Seasonal cycling in the gut microbiome of the Hadza hunter-gatherers of Tanzania. Science *357*, 802–806. https://doi.org/10.1126/science.aan4834.

32. Obregon-Tito, A.J., Tito, R.Y., Metcalf, J., Sankaranarayanan, K., Clemente, J.C., Ursell, L.K., Zech Xu, Z., Van Treuren, W., Knight, R., Gaffney, P.M., et al. (2015). Subsistence strategies in traditional societies distinguish gut microbiomes. Nat. Commun. *6*, 6505. https://doi.org/10.1038/ncomms7505.

33. Groussin, M., Poyet, M., Sistiaga, A., Kearney, S.M., Moniz, K., Noel, M., Hooker, J., Gibbons, S.M., Segurel, L., Froment, A., et al. (2021). Elevated rates of horizontal gene transfer in the industrialized human microbiome. Cell *184*, 2053–2067.e18. https://doi.org/10.1016/j.cell.2021.02.052.

34. Brewster, R., Tamburini, F.B., Asiimwe, E., Oduaran, O., Hazelhurst, S., and Bhatt, A.S. (2019). Surveying Gut Microbiome Research in Africans: Toward Improved Diversity and Representation. Trends Microbiol. *27*, 824–835. https://doi.org/10.1016/j.tim.2019.05.006.

35. Schnorr, S.L., Candela, M., Rampelli, S., Centanni, M., Consolandi, C., Basaglia, G., Turroni, S., Biagi, E., Peano, C., Severgnini, M., et al. (2014). Gut microbiome of the Hadza hunter-gatherers. Nat. Commun. *5*, 3654. https://doi.org/10.1038/ncomms4654.

36. Hansen, M.E.B., Rubel, M.A., Bailey, A.G., Ranciaro, A., Thompson, S.R., Campbell, M.C., Beggs, W., Dave, J.R., Mokone, G.G., Mpoloka, S.W., et al. (2019). Population structure of human gut bacteria in a diverse cohort from rural Tanzania and Botswana. Genome Biol. *20*, 16. https://doi.org/10.1186/s13059-018-1616-9.

37. Buttorff, C., Ruder, T., and Bauman, M. (2017). Multiple Chronic Conditions in the United States (Santa Monica, CA: RAND Corporation), pp. 5–12.

38. World Health Organization (WHO) (2022). Noncommunicable diseases (Geneva: World Health Organization). https://www.who.int/news-room/fact-sheets/detail/noncommunicable-diseases.

39. Centers for Disease Control and Prevention (CDC), National Center for Chronic Disease Prevention, and Health Promotion, (NCCDPHP). (2023). Health and economic costs of chronic diseases (Atlanta, GA: Centers for Disease Control and Prevention). https://www.cdc.gov/chronicdisease/about/costs/index.html.

40. Vargas-Robles, D., Magris, M., Morales, N., de Koning, M.N.C., Rodríguez, I., Nieves, T., Godoy-Vitorino, F., Sánchez, G.I., Alcaraz, L.D., Forney, L.J., et al. (2018). High Rate of Infection by Only Oncogenic Human Papillomavirus in Amerindians. mSphere *3*, e00176-18. https://doi.org/10.1128/mSphere.00176-18.

41. Vangay, P., Johnson, A.J., Ward, T.L., Al-Ghalith, G.A., Shields-Cutler, R.R., Hillmann, B.M., Lucas, S.K., Beura, L.K., Thompson, E.A., Till, L.M., et al. (2018). US Immigration Westernizes the Human Gut Microbiome. Cell *175*, 962–972.e10. https://doi.org/10.1016/j.cell.2018.10.029.

42. Merrill, B.D., Carter, M.M., Olm, M.R., Dahan, D., Tripathi, S., Spencer, S.P., Yu, B., Jain, S., Neff, N., Jha, A.R., et al. (2022). Ultra-deep Sequencing of Hadza Hunter-Gatherers Recovers Vanishing Gut Microbes. bioRxiv. https://doi.org/10.1101/2022.03.30.486478.

43. Tett, A., Huang, K.D., Asnicar, F., Fehlner-Peach, H., Pasolli, E., Karcher, N., Armanini, F., Manghi, P., Bonham, K., Zolfo, M., et al. (2019). The Prevotella copri Complex Comprises Four Distinct Clades Underrepresented in Westernized Populations. Cell Host Microbe *26*, 666–679.e7. https://doi.org/10.1016/j.chom.2019.08.018.

44. Thingholm, L.B., Bang, C., Rühlemann, M.C., Starke, A., Sicks, F., Kaspari, V., Jandowsky, A., Frölich, K., Ismer, G., Bernhard, A., et al. (2021). Ecology impacts the decrease of Spirochaetes and Prevotella in the fecal gut microbiota of urban humans. BMC Microbiol. *21*, 276. https://doi.org/10.1186/s12866-021-02337-5.

45. Prasoodanan P K, V., Sharma, A.K., Mahajan, S., Dhakan, D.B., Maji, A., Scaria, J., and Sharma, V.K. (2021). Western and non-western gut microbiomes reveal new roles of Prevotella in carbohydrate metabolism and mouth-gut axis. NPJ Biofilms Microbiomes *7*, 77. https://doi.org/10.1038/s41522-021-00248-x.

46. Angelakis, E., Bachar, D., Yasir, M., Musso, D., Djossou, F., Gaborit, B., Brah, S., Diallo, A., Ndombe, G.M., Mediannikov, O., et al. (2019). Treponema species enrich the gut microbiota of traditional rural populations but are absent from urban individuals. New Microbes New Infect. *27*, 14–21. https://doi.org/10.1016/j.nmni.2018.10.009.

47. Wibowo, M.C., Yang, Z., Borry, M., Hübner, A., Huang, K.D., Tierney, B.T., Zimmerman, S., Barajas-Olmos, F., Contreras-Cubas, C., García-Ortiz, H., et al. (2021). Reconstruction of ancient microbial genomes from the human gut. Nature *594*, 234–239. https://doi.org/10.1038/s41586-021-03532-0.

48. van der Vossen, E.W.J., Davids, M., Bresser, L.R.F., Galenkamp, H., van den Born, B.J.H., Zwinderman, A.H., Levin, E., Nieuwdorp, M., and de Goffau, M.C. (2023). Gut microbiome transitions across generations in different ethnicities in an urban setting-the HELIUS study. Microbiome *11*, 99. https://doi.org/10.1186/s40168-023-01488-z.

49. Geirnaert, A., Calatayud, M., Grootaert, C., Laukens, D., Devriese, S., Smagghe, G., De Vos, M., Boon, N., and Van de Wiele, T. (2017). Butyrate-producing bacteria supplemented in vitro to Crohn's disease patient microbiota increased butyrate production and enhanced intestinal epithelial barrier integrity. Sci. Rep. *7*, 11450. https://doi.org/10.1038/s41598-017-11734-8.

50. Mueller, N.T., Bakacs, E., Combellick, J., Grigoryan, Z., and Dominguez-Bello, M.G. (2015). The infant microbiome development: mom matters. Trends Mol. Med. *21*, 109–117. https://doi.org/10.1016/j.molmed.2014.12.002.

51. Cox, L.M., Yamanishi, S., Sohn, J., Alekseyenko, A.V., Leung, J.M., Cho, I., Kim, S.G., Li, H., Gao, Z., Mahana, D., et al. (2014). Altering the Intestinal Microbiota during a Critical Developmental Window Has Lasting Metabolic Consequences. Cell *158*, 705–721. https://doi.org/10.1016/j.cell.2014.05.052.

52. Zhang, X.S., Yin, Y.S., Wang, J., Battaglia, T., Krautkramer, K., Li, W.V., Li, J., Brown, M., Zhang, M., Badri, M.H., et al. (2021). Maternal cecal microbiota transfer rescues early-life antibiotic-induced enhancement of type 1 diabetes in mice. Cell Host Microbe *29*, 1249–1265.e9. https://doi.org/10.1016/j.chom.2021.06.014.

53. Sevelsted, A., Stokholm, J., and Bisgaard, H. (2016). Risk of Asthma from Cesarean Delivery Depends on Membrane Rupture. J. Pediatr. *171*, 38–42.e424. https://doi.org/10.1016/j.jpeds.2015.12.066.

54. Brown, K., Godovannyi, A., Ma, C., Zhang, Y., Ahmadi-Vand, Z., Dai, C., Gorzelak, M.A., Chan, Y., Chan, J.M., Lochner, A., et al. (2016). Prolonged antibiotic treatment induces a diabetogenic intestinal microbiome that accelerates diabetes in NOD mice. The ISME journal *10*, 321–332. https://doi.org/10.1038/ismej.2015.114.

55. Gregory, G.A., Robinson, T.I.G., and Linklater, S.E. (2022). Global incidence, prevalence, and mortality of type 1 diabetes in 2021 with projection to 2040: a modelling study (vol 10, pg 741, 2022). Lancet Diabetes Endo *10*, E11.

56. Costa, F.R.C., Françozo, M.C.S., de Oliveira, G.G., Ignacio, A., Castoldi, A., Zamboni, D.S., Ramos, S.G., Câmara, N.O., de Zoete, M.R., Palm, N.W., et al. (2016). Gut microbiota translocation to the pancreatic lymph nodes triggers NOD2 activation and contributes to T1D onset. J. Exp. Med. *213*, 1223–1239. https://doi.org/10.1084/jem.20150744.

57. Hales, C.M., Carroll, M.D., Fryar, C.D., and Ogden, C.L. (2020). Prevalence of Obesity and Severe Obesity Among Adults: United States, 2017-2018 (NCHS data brief PMID - 32487284), pp. 1–8.

58. Fryar, C.D., Carroll, M.D., and Afful, J. (2020). Prevalence of Overweight, Obesity, and Severe Obesity Among Children and Adolescents Aged 2–19 Years: United States, 1963–1965 through 2017–2018 (NCHS Health E-Stats).

59. Oksanen, J., Simpson, G.L., Blanchet, F.G., Kindt, R., Legendre, P., Minchin, P.R., O'Hara, R.B., Solymos, P., Stevens, M.H.H., Szoecs, E., and Wagner, H. (2022). vegan: Community Ecology Package (R package version 2.6-4). https://cran.r-project.org/package=vegan.

60. Paradis, E., Blomberg, S., Bolker, B., Brown, J., Claramunt, S., Claude, J., Cuong, H.S., Desper, R., Didier, G., Durand, B., et al. (2024). Analyses of Phylogenetics and Evolution. Bioinformatics *35*, 526–528. https://doi.org/10.1093/bioinformatics/bty633.

61. Pedersen T.L. (2025) ggraph: An Implementation of Grammar of Graphics for Graphs and Networks. CRAN: Package. https://doi.org/10.32614/CRAN.package.ggraph.

62. Thompson, L.R., Sanders, J.G., McDonald, D., Amir, A., Ladau, J., Locey, K.J., Prill, R.J., Tripathi, A., Gibbons, S.M., Ackermann, G., et al. (2017). A communal catalogue reveals Earth's multiscale microbial diversity. Nature *551*, 457–463. https://doi.org/10.1038/nature24621.

63. Caporaso, J.G., Kuczynski, J., Stombaugh, J., Bittinger, K., Bushman, F.D., Costello, E.K., Fierer, N., Peña, A.G., Goodrich, J.K., Gordon, J.I., et al. (2010). QIIME allows analysis of high-throughput community sequencing data. Nat. Methods *7*, 335–336. https://doi.org/10.1038/nmeth.f.303.

64. Callahan, B.J., McMurdie, P.J., Rosen, M.J., Han, A.W., Johnson, A.J.A., and Holmes, S.P. (2016). DADA2: High-resolution sample inference from Illumina amplicon data. Nat. Methods *13*, 581–583. https://doi.org/10.1038/nmeth.3869.

65. Bokulich, N.A., Kaehler, B.D., Rideout, J.R., Dillon, M., Bolyen, E., Knight, R., Huttley, G.A., and Gregory Caporaso, J. (2018). Optimizing taxonomic classification of marker-gene amplicon sequences with QIIME 2's q2-feature-classifier plugin. Microbiome *6*, 90. https://doi.org/10.1186/s40168-018-0470-z.

66. Glöckner, F.O., Yilmaz, P., Quast, C., Gerken, J., Beccati, A., Ciuprina, A., Bruns, G., Yarza, P., Peplies, J., Westram, R., and Ludwig, W. (2017). 25 years of serving the community with ribosomal RNA gene reference databases and tools. J. Biotechnol. *261*, 169–176. https://doi.org/10.1016/j.jbiotec.2017.06.1198.

67. Faith, D.P. (1992). Conservation evaluation and phylogenetic diversity. Biol. Conserv. *61*, 1–10.

68. Lozupone, C.A., Hamady, M., Kelley, S.T., and Knight, R. (2007). Quantitative and Qualitative β Diversity Measures Lead to Different Insights into Factors That Structure Microbial Communities. Appl. Environ. Microbiol. *73*, 1576–1585. https://doi.org/10.1128/AEM.01996-06.

69. Clarke, E.L., Taylor, L.J., Zhao, C., Connell, A., Lee, J.J., Fett, B., Bushman, F.D., and Bittinger, K. (2019). Sunbeam: an extensible pipeline for analyzing metagenomic sequencing experiments. Microbiome *7*, 46. https://doi.org/10.1186/s40168-019-0658-x.

70. Wood, D.E., and Salzberg, S.L. (2014). Kraken: ultrafast metagenomic sequence classification using exact alignments. Genome Biol. *15*, R46. https://doi.org/10.1186/gb-2014-15-3-r46.

71. Ogata, H., Goto, S., Sato, K., Fujibuchi, W., Bono, H., and Kanehisa, M. (1999). KEGG: Kyoto Encyclopedia of Genes and Genomes. Nucleic Acids Res. *27*, 29–34. https://doi.org/10.1093/nar/27.1.29.

72. Buchfink, B., Xie, C., and Huson, D.H. (2015). Fast and sensitive protein alignment using DIAMOND. Nat. Methods *12*, 59–60. https://doi.org/10.1038/nmeth.3176.

73. Bushman, F.D., Conrad, M., Ren, Y., Zhao, C., Gu, C., Petucci, C., Kim, M.S., Abbas, A., Downes, K.J., Devas, N., et al. (2020). Multi-omic Analysis of the Interaction between Clostridioides difficile Infection and Pediatric Inflammatory Bowel Disease. Cell Host Microbe *28*, 422–433.e7. https://doi.org/10.1016/j.chom.2020.07.020.

74. Denburg, M.R., Koepsell, K., Lee, J.J., Gerber, J., Bittinger, K., and Tasian, G.E. (2020). Perturbations of the Gut Microbiome and Metabolome in Children with Calcium Oxalate Kidney Stone Disease. J. Am. Soc. Nephrol. *31*, 1358–1369. https://doi.org/10.1681/ASN.2019101131.

75. Polster, S.P., Sharma, A., Tanes, C., Tang, A.T., Mericko, P., Cao, Y., Carrión-Penagos, J., Girard, R., Koskimäki, J., Zhang, D., et al. (2020). Permissive microbiome characterizes human subjects with a neurovascular disease cavernous angioma. Nat. Commun. *11*, 2659. https://doi.org/10.1038/s41467-020-16436-w.

76. Ling, W., Lu, J., Zhao, N., Lulla, A., Plantinga, A.M., Fu, W., Zhang, A., Liu, H., Song, H., Li, Z., et al. (2022). Batch effects removal for microbiome data via conditional quantile regression. Nat. Commun. *13*, 5418. https://doi.org/10.1038/s41467-022-33071-9.

77. Seedorf, H., Kittelmann, S., and Janssen, P.H. (2015). Few highly abundant operational taxonomic units dominate within rumen methanogenic archaeal species in New Zealand sheep and cattle. Appl. Environ. Microbiol. *81*, 986–995. https://doi.org/10.1128/aem.03018-14.

78. Weinert-Nelson, J.R., Biddle, A.S., Sampath, H., and Williams, C.A. (2023). Fecal Microbiota, Forage Nutrients, and Metabolic Responses of Horses Grazing Warm- and Cool-Season Grass Pastures. Animals. *13*, 790. https://doi.org/10.3390/ani13050790.

79. Honarbakhsh, M., Ericsson, A., Zhong, G., Isoherranen, N., Zhu, C., Bromberg, Y., Van Buiten, C., Malta, K., Joseph, L., Sampath, H., et al. (2021). Impact of vitamin A transport and storage on intestinal retinoid homeostasis and functions. J. Lipid Res. *62*, 100046. https://doi.org/10.1016/j.jlr.2021.100046.

80. Scanlan, P.D., Stensvold, C.R., Rajilić-Stojanović, M., Heilig, H.G.H.J., De Vos, W.M., O'Toole, P.W., and Cotter, P.D. (2014). The microbial eukaryote Blastocystis is a prevalent and diverse member of the healthy human gut microbiota. FEMS Microbiol. Ecol. *90*, 326–330. https://doi.org/10.1111/1574-6941.12396.

81. Scicluna, S.M., Tawari, B., and Clark, C.G. (2006). DNA barcoding of blastocystis. Protist *157*, 77–85. https://doi.org/10.1016/j.protis.2005.12.001.

82. Jolley, K.A., and Maiden, M.C.J. (2010). BIGSdb: Scalable analysis of bacterial genome variation at the population level. BMC Bioinf. *11*, 595. https://doi.org/10.1186/1471-2105-11-595.

83. Scanlan, P.D., Stensvold, C.R., and Cotter, P.D. (2015). Development and Application of a Blastocystis Subtype-Specific PCR Assay Reveals that Mixed-Subtype Infections Are Common in a Healthy Human Population. Appl. Environ. Microbiol. *81*, 4071–4076. https://doi.org/10.1128/AEM.00520-15.

84. Kaul, A., Mandal, S., Davidov, O., and Peddada, S.D. (2017). Analysis of Microbiome Data in the Presence of Excess Zeros. Front. Microbiol. *8*, 2114. https://doi.org/10.3389/fmicb.2017.02114.

85. Kurtz, Z.D., Müller, C.L., Miraldi, E.R., Littman, D.R., Blaser, M.J., and Bonneau, R.A. (2015). Sparse and Compositionally Robust Inference of Microbial Ecological Networks. PLoS Comput. Biol. *11*, e1004226. https://doi.org/10.1371/journal.pcbi.1004226.

STAR★METHODS

KEY RESOURCES TABLE

REAGENT or RESOURCE	SOURCE	IDENTIFIER
Biological samples		
Healthy volunteer fecal, oral, nasal, skin samples from Amazon	This paper	N/A
Critical commercial assays		
DNeasy PowerSoil HTP 96	QIAGEN	12955–4
Platinum Hot Start PCR Master Mix	ThermoFisher	13000013
Quant-it PicoGreen dsDNA assay	ThermoFisher	P7589
Qubit dsDNA HS Assay Kit	ThermoFisher	Q32854
Quantinova SYBR green PCR kit	QIAGEN	208252
Deposited data		
All 16S and shotgun metagenomic sequences	This paper	ENA: PRJEB55648
Previously sequenced cohort (US children)	https://doi.org/10.1016/j.chom.2020.07.020	ENA: PRJNA562600
Previously sequenced cohort (US adult)	https://doi.org/10.1038/s41467-020-16436-w	ENA: PRJNA629755
Previously 16S sequences from American Gut Project cohort	https://doi.org/10.1128/msystems.00031-18	ENA: PRJEB11419
Previously 16S sequences from Hadza cohort	https://doi.org/10.1126/science.aan4834	ENA: PRJEB27517
Oligonucleotides		
16S rRNA forward primer 515F (AATGATACGGCGACCACCGAGATCTAC ACGCT XXXXXXXXXXX TATGGTAATT GT GTGYCAGCMGCCGCGGTAA)	Integrated DNA Technologies	N/A
16S rRNA reverse primer 806R (CAAGCAGAAGACGGCATACGAGAT AGTCAGCCAG CC GGACTA CNVGGGTWTCTAAT)	Integrated DNA Technologies	N/A
Total Bacteria QPCR forward primer (ACTCCTACGGGAGGCAGCAG)	Integrated DNA Technologies	N/A
Total Bacteria QPCR reverse primer (ATTACCGCGGCTGCTGG)	Integrated DNA Technologies	N/A
Methanobrevibacter smithii QPCR forward primer (AAGGATTTGCACCCAACAC)	Integrated DNA Technologies	N/A
Methanobrevibacter smithii QPCR reverse primer (GACCACAGTTAGGACCCTCTGG)	Integrated DNA Technologies	N/A
Software and algorithms		
QIIME2 2018.4.0	https://doi.org/10.1038/nmeth.f.303	https://qiime2.org/
R V4.2.2	https://www.r-project.org/	https://www.r-project.org/
sunbeam V2.1.0	https://doi.org/10.1186/s40168-019-0658-x	https://github.com/sunbeam-labs/sunbeam
ConQuR V1.2.0	https://doi.org/10.1038/s41467-022-33071-9	https://github.com/wdl2459/ConQuR
ANCOM V2.1	https://doi.org/10.3402/mehd.v26.27663	https://github.com/FrederickHuangLin/ANCOM-Code-Archive
SpiecEasi V1.1.1	https://doi.org/10.1371/journal.pcbi.1004226	https://github.com/zdk123/SpiecEasi
vegan R package V2.6-4	Oksanen et al.[59]	https://cran.r-project.org/web/packages/vegan/index.html

(*Continued on next page*)

Continued

REAGENT or RESOURCE	SOURCE	IDENTIFIER
ape R package V5.7-1	Paradis et al.[60]	https://cran.r-project.org/web/packages/ape/index.html
ggraph R package V2.1.0	Pedersen et al.[61]	https://cran.r-project.org/web/packages/ggraph/index.html
tidyverse R package V2.0.0	https://doi.org/10.21105/joss.01686	https://tidyverse.org/packages/

EXPERIMENTAL MODEL AND STUDY PARTICIPANT DETAILS

Subjects and samples

This study was approved by the communities and by the Ethical Review Board of the Venezuelan Institute for Scientific Research (IVIC-DIR-0021/1582/2017), and individuals provided their consent to participate at each sampling time. Amerindians from Yek'wana and Yanomami-Sanema villages in a region of 100 sq Km in the Southern Bolivar State of Venezuela were recruited. Seven remote, low-exposure villages were integrated into the OEPA program in 2015. One nonendemic village with medium exposure to Western visitors and medicines was included in the study as a reference for long-term exposure to medicines. The village has a medical post supplying medicines, antibiotics, antiparasitic drugs, and vaccines.

In total, 118 subjects from low-exposure villages and 79 subjects from medium-exposure villages were recruited in 2015, before the low-exposure villages started Ivermectin treatment; 161 subjects from low-exposure villages and 74 subjects from medium-exposure villages were recruited in 2016, after all villages received Ivermectin treatment (see Table S5 for details). Samples were taken from the nose, mouth, skin (on the right arm and right hand), and feces by swabbing, and were immediately frozen in dry shippers in the field.

OEPA villages receive quarterly medical visits to screen for the parasite and administer Ivermectin to villagers older than 4 years of age (dose of 150 μg per kilogram of body weight) in accordance with the OEPA protocols[9],[43] In addition to ivermectin, health workers also offered medical services and provided medicines, most commonly vaccines, amoxicillin, analgesics, antifungals, anti-inflammatories, and vitamins.

METHOD DETAILS

Library preparation and sequencing

Microbial DNA was extracted from collected samples using Qiagen DNeasy PowerSoil HTP 96 Kit following the manufacturer's instructions. The V4 region of *16S rRNA* gene was amplified using the 515F/806R primers according to the EMP protocol (https://earthmicrobiome.org/).[62] Prepared amplicon libraries were sequenced using Illumina MiSeq sequencing instrument. Shotgun metagenomic sequencing was performed on fecal DNA and library was prepared using Nextera or NEBNext. Sequencing was performed at Children's Hospital of Philadelphia Microbiome Center (Philadelphia, PA, USA) or at Genewiz, LLC. (South Plainfield, NJ, USA).

16S rRNA sequencing data processing

Raw reads were de-multiplexed, and quality filtered using QIIME2 2018.4.0.[63] Quality-filtered reads were clustered into amplicon sequence variants (ASVs) using DADA2.[64] Taxonomic classification of these ASVs was obtained with q2-feature-classifier plugin[65] with the SILVA ribosomal RNA database[66] v132 as a reference. For comparison between samples with difference sequencing depth, ASV counts were rarefied to 10,000 reads per sample. Faith's Phylogenetic Diversity,[67] observed ASV, Pielou evenness, and Shannon indices were calculated for α-diversity metrics. Unweighted/weighted UniFrac distances[68] and Bray-Curtis similarity were calculated for β-diversity.

Beta diversity analysis for Figure 3A was based on *16S rRNA* gene amplicon data from 342 fecal samples in this study and publicly available reference datasets, including industrialized populations from the American Gut Project (Australia, Canada, Mexico, United Kingdom, and United States; ENA PRJEB11419) and a non-industrialized Hadza hunter-gatherer cohort from Tanzania (ENA PRJEB27517). All datasets were processed using a harmonized pipeline, Bray–Curtis dissimilarities were computed on relative abundance data, and patterns were visualized by principal coordinate analysis (PCoA), with population differences along PC1 assessed by Kruskal–Wallis tests.

Shotgun metagenomic sequencing data processing

Shotgun metagenomic data were analyzed using Sunbeam, a user-extendable bioinformatics pipeline that we developed for this purpose.[69] Quality control steps were performed by the default workflows in Sunbeam, which are optimized to remove host-derived sequences and reads of low sequence complexity. The abundance of bacteria was estimated using Kraken.[70] Reads were mapped to the KEGG database[71] using Diamond[72] to estimate the abundance of bacterial gene orthologs. Sample similarities were assessed by Bray-Curtis and Jaccard distances. Metagenomic shotgun data of healthy US subjects are used from previously published study

sequenced at Children's Hospital of Philadelphia Microbiome Center, children (n = 74, age range 0–18 yr)[73,74]; adults (n = 27, 17 female, Age range 21–78 yr),[75] as control. To correct batch effects of the shotgun metagenomic data from two facilities, we used ConQuR[76] to adjust the gene count table from Genewiz sequencing data.

Quantitative real-time PCR of methanogens

Copy numbers of *Methanobrevibacter smithii* were measured using quantitative PCR with specific primers (Fwd-AAGGATTTGCACCCAACAC, Rev-GACCACAGTTAGGACCCTCTGG). The real-time PCR grogram started with an initial step at 95 for 10 min, followed by 40 cycles of 10 s at 95 C, 30 s at 57 C, 20 s at 72 C.[77] The copy numbers were normalized by total bacteria copy numbers with universal primer (Fwd-ACTCCTACGGGAGGCAGCAG, Rev-ATTACCGCGGCTGCTGG). The real-time PCR grogram for total bacteria is initial at 95 for 5 min, followed by 45 cycles of 10 s at 95 C, 10 s at 60 C, 10 s at 72 C. Real-time PCR was performed using a Quantstudio 3 system (Thermo Fisher, Waltham, MA, USA) with Quantinova SYBR green PCR kit (Qiagen, Hilden, Germany), 1 μL of extracted DNA were added as templates, genomic DNA with known copy numbers were used as the standards.

Fecal volatile fatty acid analysis

Fecal volatile fatty acid (VFA, including acetate, propionate, butyrate, valerate, isobutyrate and isovalerate) concentrations were determined by GC-MS analysis. Sample preparation was performed as described.[78] In brief, frozen fecal samples were weighed and load into bead tubes, then resuspended in 1 mL of 0.5% phosphoric acid per 0.1 g of samples and samples were homogenized and then centrifuged (10 min at 17,949xg). The aqueous fecal suspensions were extracted with diethyl ether (1:1, vol:vol). Before analysis, 2-methyl hexanoic acid (Thermo Fisher Scientific, Dallas, TX, USA) was added to the organic phase extract as an internal standard. Samples were analyzed in duplicate, with independent extractions for each replicate. The procedures for VFA quantitation have been previously described by Honarbakhsh et al.[79]

Intestinal parasites detection

Microscopic parasite detection was performed on fecal suspensions in the field, by a clinical laboratory technologist. Fecal *Blastocystis* sp was detected by PCR amplification on fecal DNA, and subtype classification was performed by allele barcoding using the primer pair RD5 and Bhr according to standard protocols.[80,81] Sequences were used to assign *Blastocystis* subtype and allele using the online database http://pubmlst.org/blastocystis.[82] Additional PCR assays were conducted to determine *Blastocystis* species richness—defined as the number of distinct subtypes present—using nested PCRs with primers targeting ST1, ST2, ST3, and ST4, as previously described.[83]

QUANTIFICATION AND STATISTICAL ANALYSIS

Microbiota diversity analyses

Linear regression models were performed to examine the effects of exposure, age, and gender on alpha diversities. Wilcox test of alpha diversity between different exposure level or between 2015 and 2016 was also performed and p-values were adjusted with FDR. Beta diversity difference between sample groups were assessed using adonis2 function in R package vegan with 999 permutations. Principal coordinate analyses (PCoA) were generated to reduce dimensions. Distance-based Redundancy Analyses (dbRDA) were performed to assess the microbial community composition change explained by exposure level or year.

Gene pathways analyses

Linear models were used to detect differences in logit-transformed gene and pathway abundance between sample groups; p-values from multiple testing procedures were corrected to control for a specified false discovery rate.

Differential taxa analyses

ANCOM[84] was used to search for determining discordant bacterial taxa by between groups at the genus (*16S rRNA data*) or species level (shotgun metagenomic data). The results were corrected by age and p-values adjusted by FDR.

Co-abundance network analyses

SparCC from SpiecEasi[85] was employed to represent co-abundance network. The pseudo p-value <0.01 were considered significant and correlation magnitudes >0.7 and < −0.7 were kept and visualized with ggraph in R.

Cell Reports, Volume *45*

Supplemental information

Rapid microbiome restructuring associated with medical exposure in remote Amazonian Indigenous communities

Haipeng Sun, Oscar Noya-Alarcon, Jincheng Wang, Scott G. Daniel, Kyle Bittinger, Wessam Mohamed, Pauline D. Scanlan, Charvi Shah, Tanima Kundu, Martin J. Blaser, Noel T. Mueller, Orlana Lander, Mariapia Bevilaqua, Daniela Vargas Robles, Monica Contreras, and Maria G. Dominguez-Bello

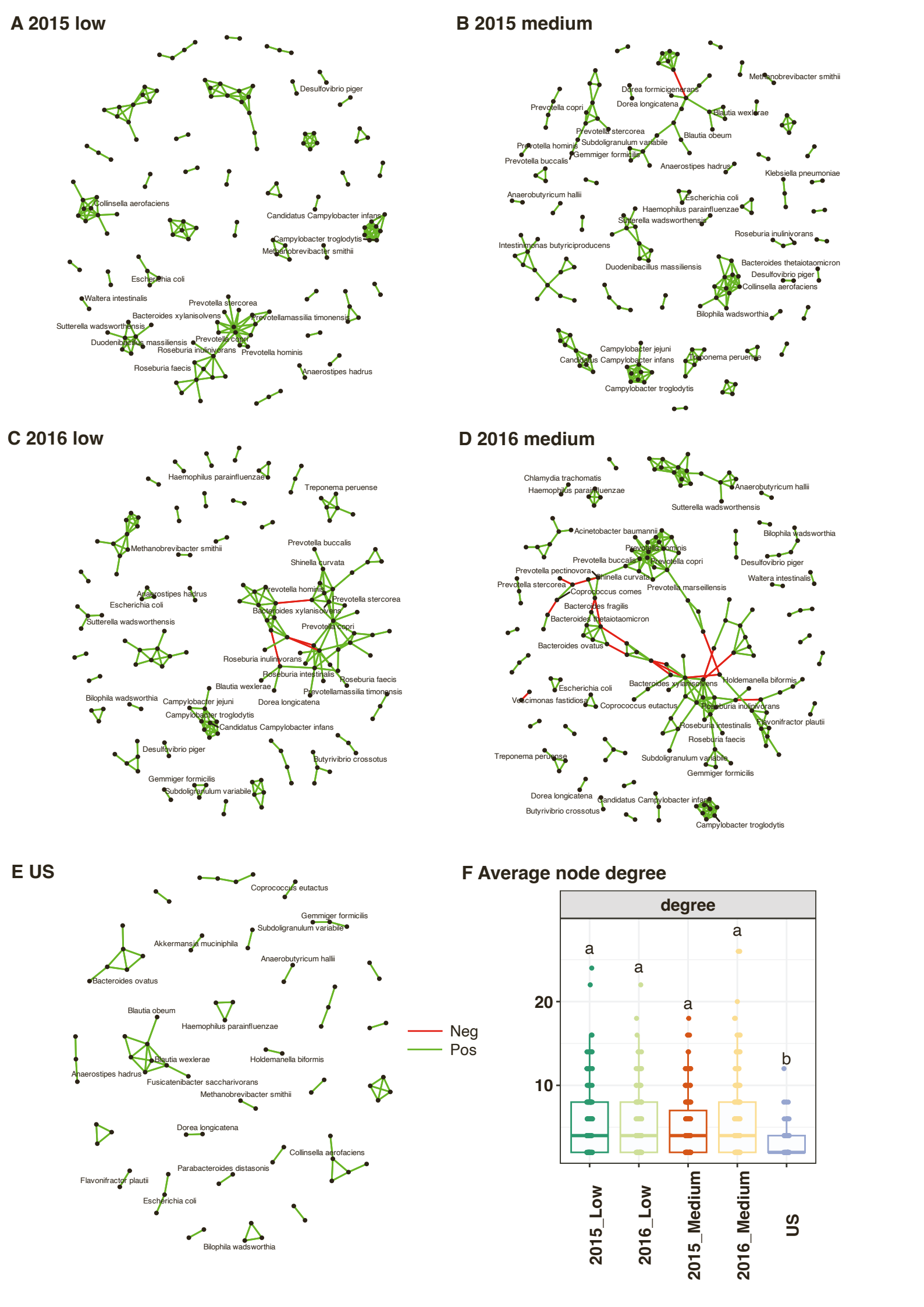

A 2015 low
Desulfovibrio piger
Collinsella aerofaciens
Candidatus Campylobacter infans
Campylobacter troglodytis
Methanobrevibacter smithii
Escherichia coli
Waltera intestinalis
Prevotella stercorea
Bacteroides xylanisolvens
Prevotellamassilia timonensis
Sutterella wadsworthensis
Duodenibacillus massiliensis
Prevotella copri
Roseburia inulinivorans
Prevotella hominis
Roseburia faecis
Anaerostipes hadrus
B 2015 medium
Methanobrevibacter smithii
Dorea formicigenerans
Dorea longicatena
Prevotella copri
Blautia wexlerae
Prevotella stercorea
Blautia obeum
Subdoligranulum variabile
Prevotella hominis
Gemmiger formicilis
Prevotella buccalis
Anaerostipes hadrus
Klebsiella pneumoniae
Anaerobutyricum hallii
Escherichia coli
Haemophilus parainfluenzae
Sutterella wadsworthensis
Roseburia inulinivorans
Intestinimonas butyriciproducens
Duodenibacillus massiliensis
Bacteroides thetaiotaomicron
Desulfovibrio piger
Collinsella aerofaciens
Bilophila wadsworthia
Campylobacter jejuni
Candidatus Campylobacter infans
Treponema peruense
Campylobacter troglodytis
C 2016 low
Haemophilus parainfluenzae
Treponema peruense
Methanobrevibacter smithii
Prevotella buccalis
Shinella curvata
Prevotella hominis
Prevotella stercorea
Anaerostipes hadrus
Escherichia coli
Bacteroides xylanisolvens
Sutterella wadsworthensis
Prevotella copri
Roseburia inulinivorans
Roseburia intestinalis
Roseburia faecis
Blautia wexlerae
Prevotellamassilia timonensis
Bilophila wadsworthia
Campylobacter jejuni
Dorea longicatena
Campylobacter troglodytis
Candidatus Campylobacter infans
Desulfovibrio piger
Butyrivibrio crossotus
Gemmiger formicilis
Subdoligranulum variabile
D 2016 medium
Chlamydia trachomatis
Haemophilus parainfluenzae
Anaerobutyricum hallii
Sutterella wadsworthensis
Acinetobacter baumannii
Bilophila wadsworthia
Prevotella hominis
Prevotella buccalis
Prevotella copri
Desulfovibrio piger
Prevotella pectinovora
Shinella curvata
Waltera intestinalis
Prevotella stercorea
Coprococcus comes
Prevotella marseillensis
Bacteroides fragilis
Bacteroides thetaiotaomicron
Bacteroides ovatus
Holdemanella biformis
Escherichia coli
Bacteroides xylanisolvens
Veillonella fastidiosa
Coprococcus eutactus
Roseburia inulinivorans
Flavonifractor plautii
Roseburia intestinalis
Roseburia faecis
Treponema peruense
Subdoligranulum variabile
Gemmiger formicilis
Dorea longicatena
Candidatus Campylobacter infans
Butyrivibrio crossotus
Campylobacter troglodytis
E US
Coprococcus eutactus
Gemmiger formicilis
Subdoligranulum variabile
Akkermansia muciniphila
Anaerobutyricum hallii
Bacteroides ovatus
Blautia obeum
Haemophilus parainfluenzae
Blautia wexlerae
Holdemanella biformis
Anaerostipes hadrus
Fusicatenibacter saccharivorans
Methanobrevibacter smithii
Dorea longicatena
Collinsella aerofaciens
Parabacteroides distasonis
Flavonifractor plautii
Escherichia coli
Bilophila wadsworthia
Neg
Pos
F Average node degree
degree
20
10
a
a
a
a
b
2015_Low
2016_Low
2015_Medium
2016_Medium
US

Figure S1. Co-occurrence network structure of the fecal microbiota; related to STAR Methods and Figure 2

Co-occurrence networks constructed from shotgun metagenomic data, stratified by urban exposure level and sampling year. Nodes represent bacterial taxa and edges represent significant co-occurrence relationships. Differences in network connectivity and node degree illustrate variation in community structure across exposure groups.

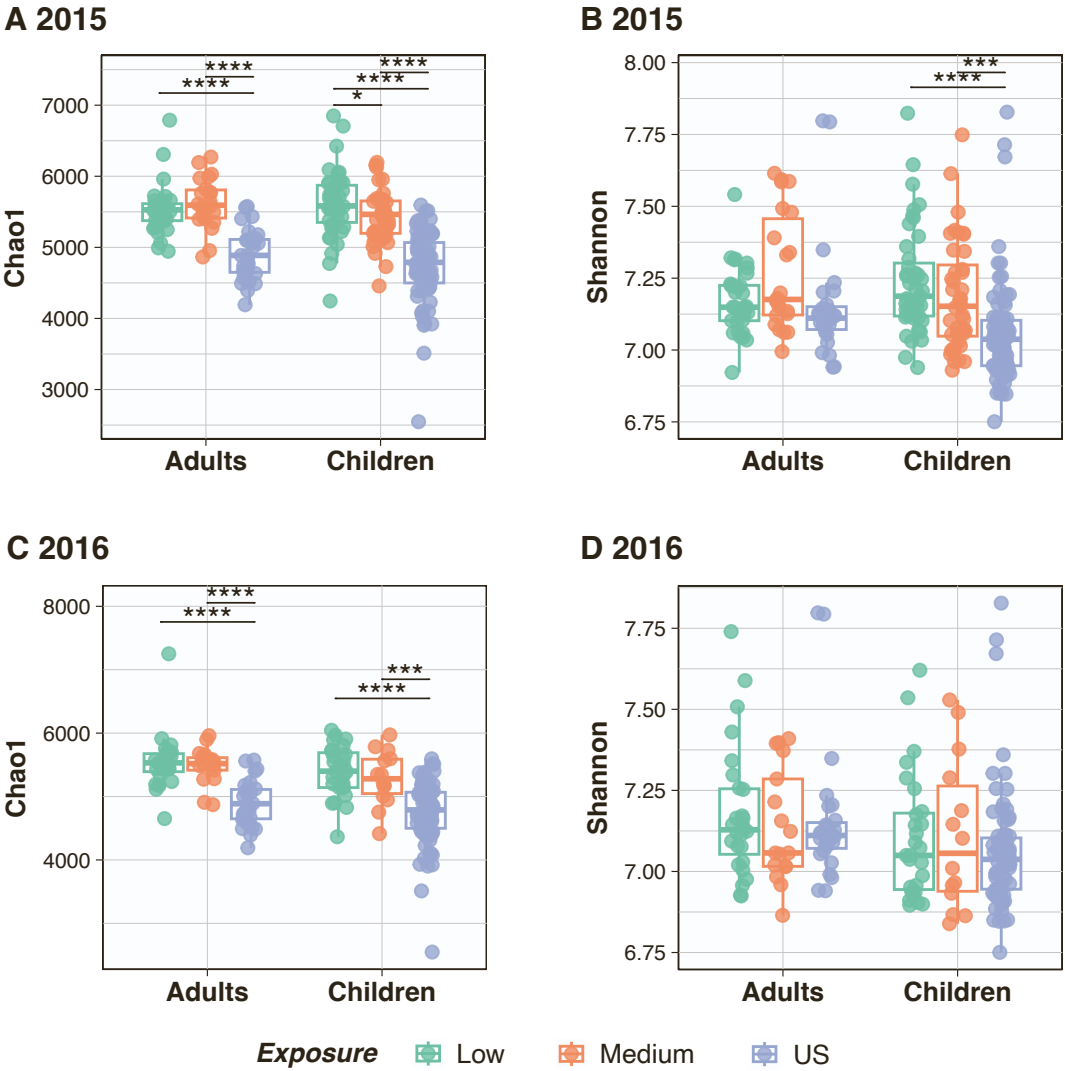
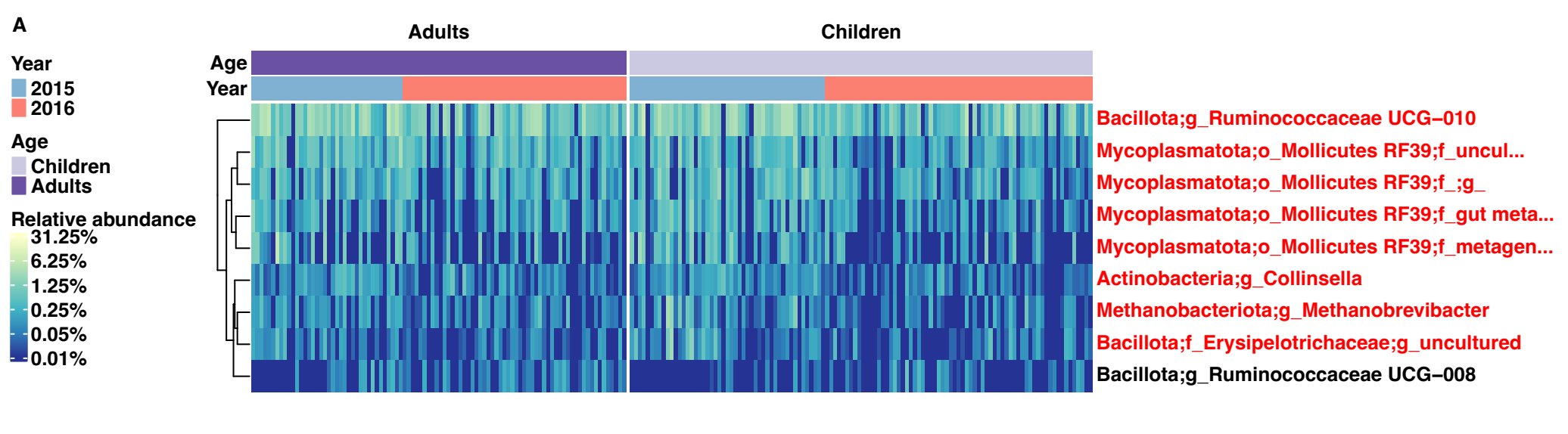

A 2015
B 2015
C 2016
D 2016
Chao1
Shannon
Adults
Children
****
***
*
Exposure
Low
Medium
US

Figure S2. Fecal α-diversity across urban exposure levels; related to STAR Methods and Figure 2

Chao1 richness estimates and Shannon diversity derived from shotgun metagenomic data across urban exposure levels. Asterisks indicate levels of statistical significance following the standard convention used throughout the figures: *$p < 0.05$; **$p < 0.01$; ***$p < 0.001$; ****$p < 0.0001$.


A
Year
2015
2016
Age
Children
Adults
Relative abundance
31.25%
6.25%
1.25%
0.25%
0.05%
0.01%
Adults
Children
Age
Year
Bacillota;g_Ruminococcaceae UCG−010
Mycoplasmatota;o_Mollicutes RF39;f_uncul...
Mycoplasmatota;o_Mollicutes RF39;f_;g_
Mycoplasmatota;o_Mollicutes RF39;f_gut meta...
Mycoplasmatota;o_Mollicutes RF39;f_metagen...
Actinobacteria;g_Collinsella
Methanobacteriota;g_Methanobrevibacter
Bacillota;f_Erysipelotrichaceae;g_uncultured
Bacillota;g_Ruminococcaceae UCG−008

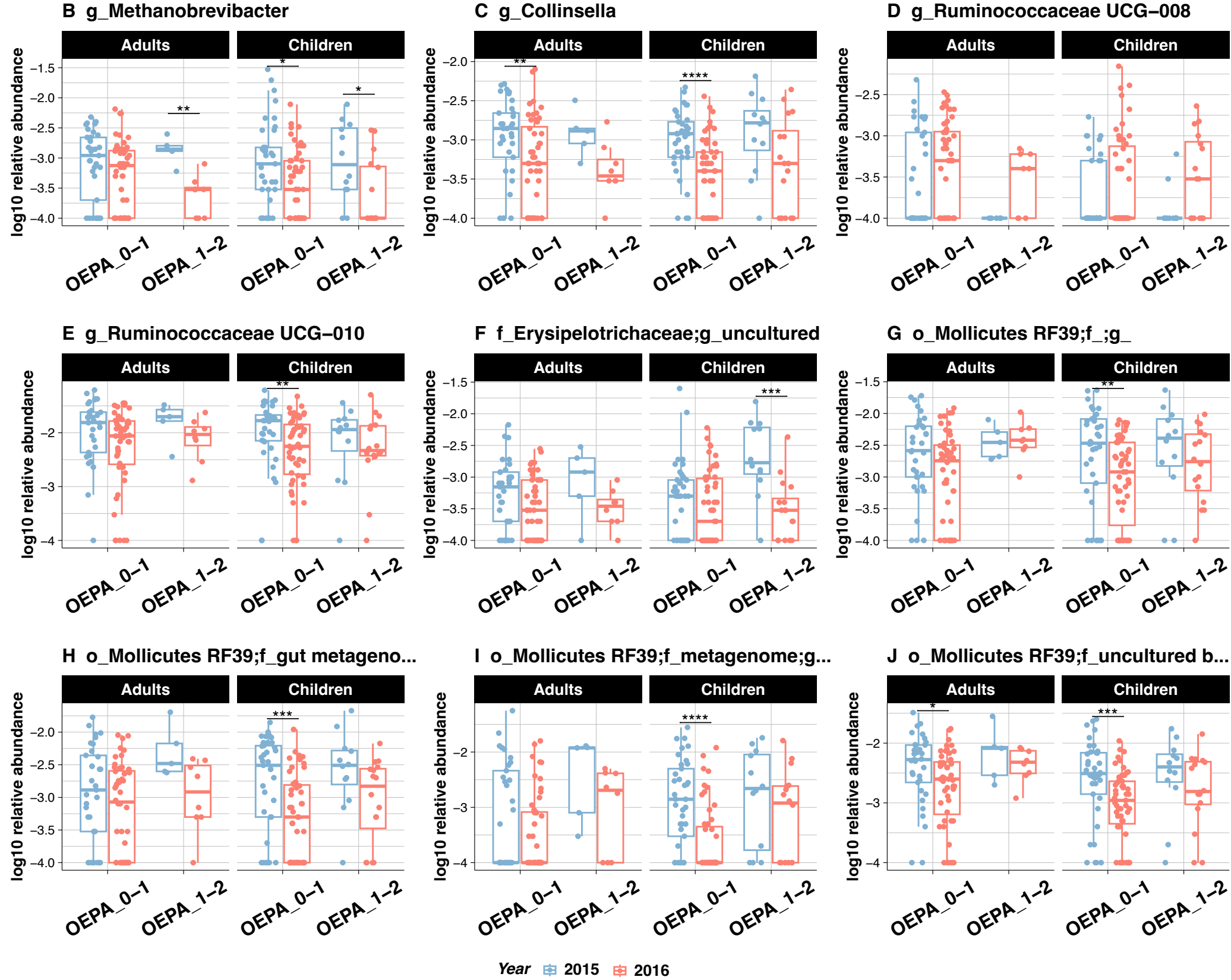
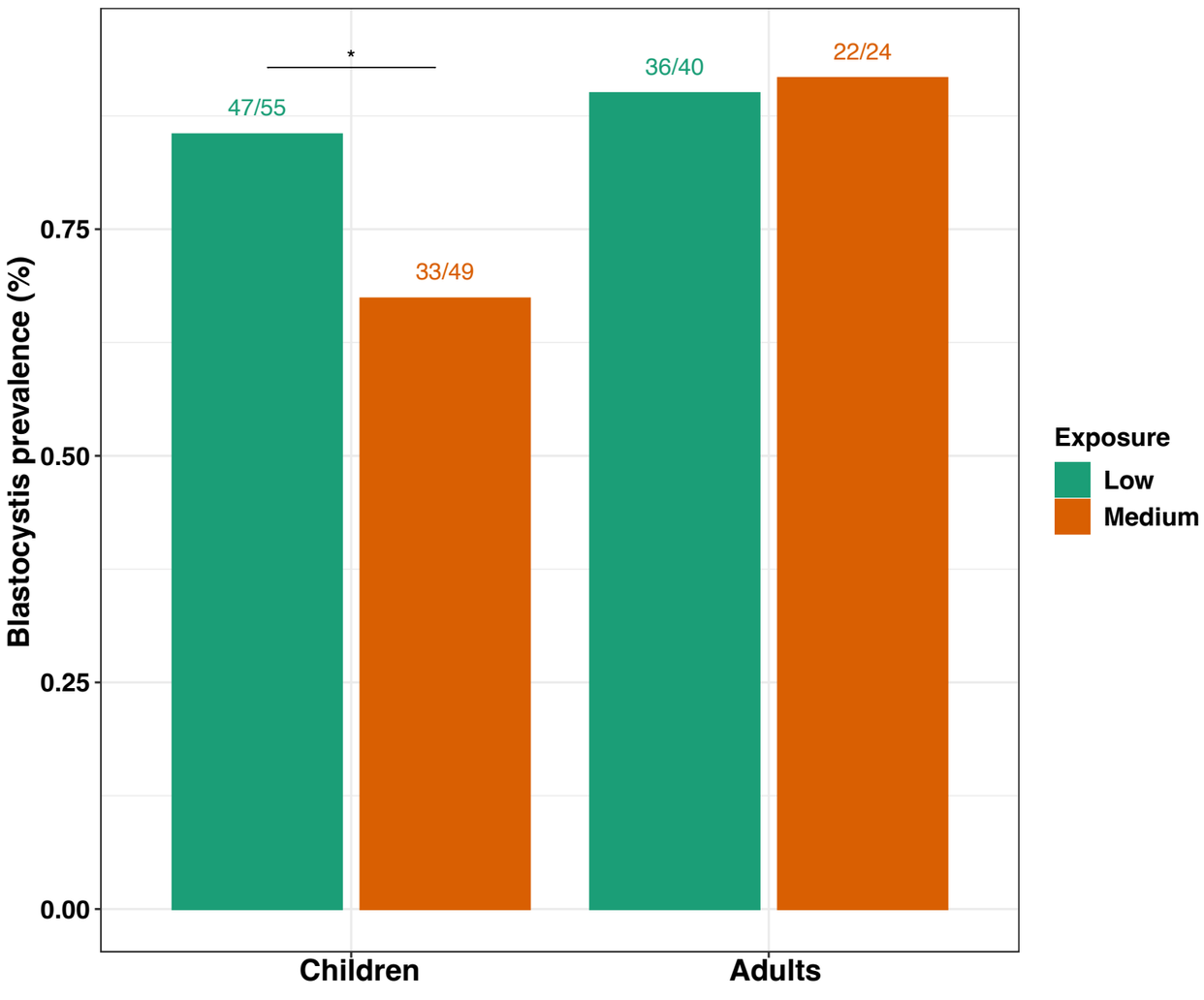

B g_Methanobrevibacter
C g_Collinsella
D g_Ruminococcaceae UCG−008
E g_Ruminococcaceae UCG−010
F f_Erysipelotrichaceae;g_uncultured
G o_Mollicutes RF39;f_;g_
H o_Mollicutes RF39;f_gut metageno...
I o_Mollicutes RF39;f_metagenome;g...
J o_Mollicutes RF39;f_uncultured b...
Adults
Children
log10 relative abundance
OEPA_0−1
OEPA_1−2
Year 2015 2016

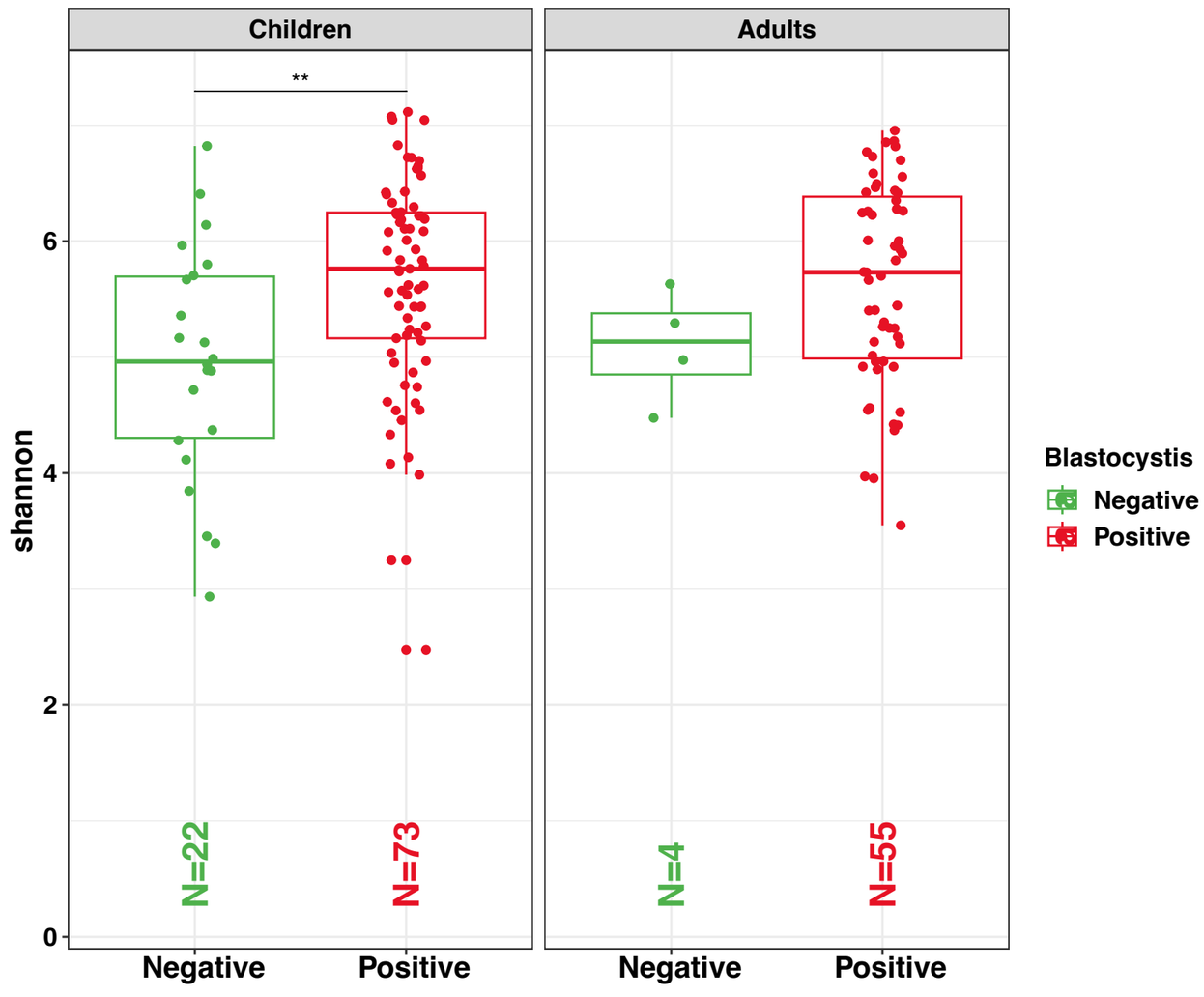
Figure S3. Differentially abundant fecal bacterial taxa between sampling years; related to STAR Methods and Figure 3

Differentially abundant fecal bacterial taxa identified by *16S rRNA* gene sequencing between the 2015 and 2016 sampling visits in low–urban-exposure villages. Taxa shown meet the statistical significance threshold (FDR-corrected $p < 0.05$). (B-J) Boxplots showing $\log_{10}$-transformed relative abundances of representative genera that changed significantly between years. Comparisons were performed using Wilcoxon rank-sum tests; FDR-adjusted *p* values are indicated:*$p < 0.05$; **$p < 0.01$; ***$p < 0.001$.

A


*
47/55
33/49
36/40
22/24
Blastocystis prevalence (%)
0.75
0.50
0.25
0.00
Children
Adults
Exposure
Low
Medium

B


Children
Adults
**
shannon
6
4
2
0
N=22
N=73
N=4
N=55
Negative
Positive
Negative
Positive
Blastocystis
Negative
Positive

C

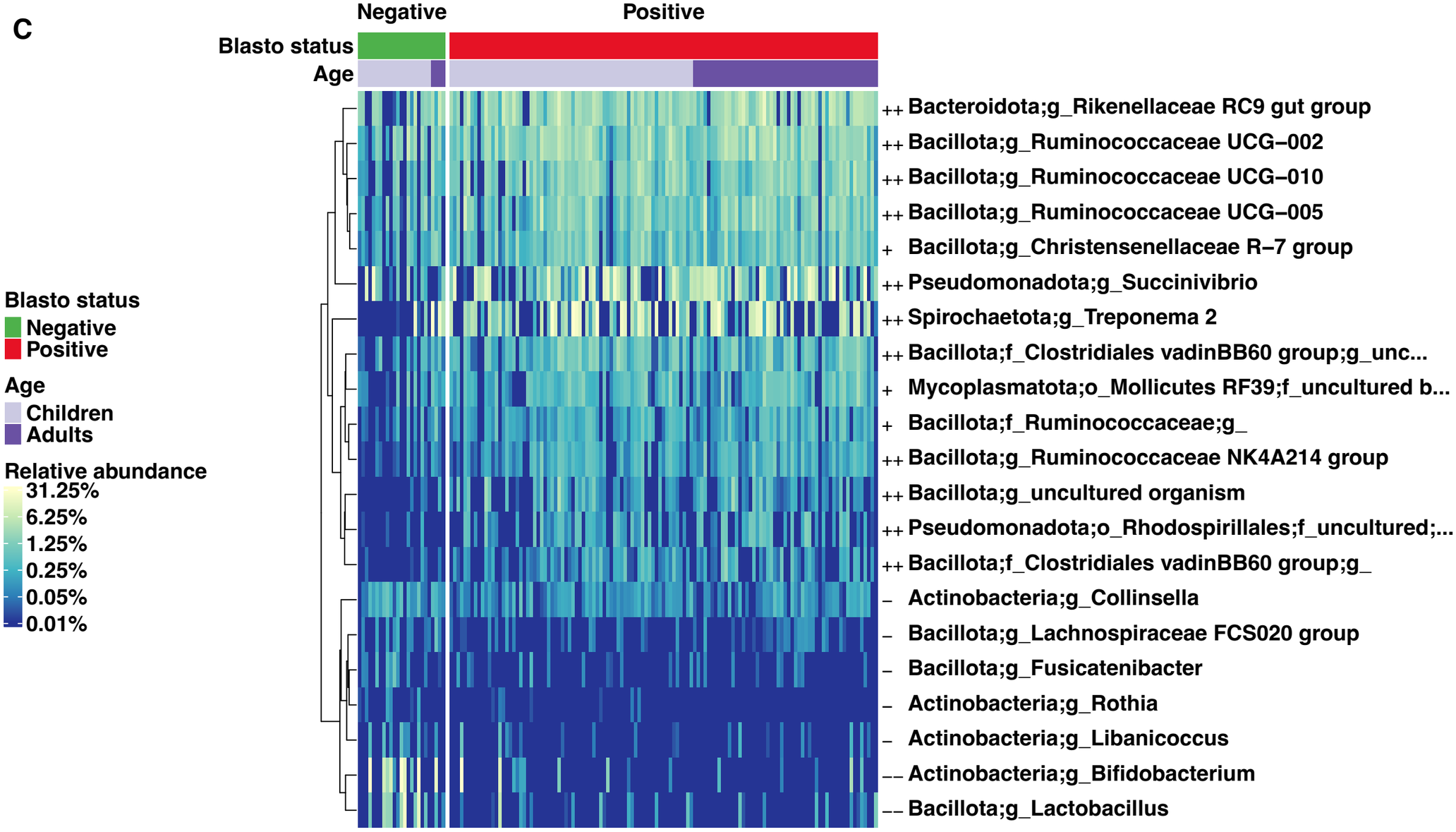

Negative
Positive
Blasto status
Age
++ Bacteroidota;g_Rikenellaceae RC9 gut group
++ Bacillota;g_Ruminococcaceae UCG–002
++ Bacillota;g_Ruminococcaceae UCG–010
++ Bacillota;g_Ruminococcaceae UCG–005
+ Bacillota;g_Christensenellaceae R–7 group
++ Pseudomonadota;g_Succinivibrio
++ Spirochaetota;g_Treponema 2
++ Bacillota;f_Clostridiales vadinBB60 group;g_unc...
+ Mycoplasmatota;o_Mollicutes RF39;f_uncultured b...
+ Bacillota;f_Ruminococcaceae;g_
++ Bacillota;g_Ruminococcaceae NK4A214 group
++ Bacillota;g_uncultured organism
++ Pseudomonadota;o_Rhodospirillales;f_uncultured;...
++ Bacillota;f_Clostridiales vadinBB60 group;g_
– Actinobacteria;g_Collinsella
– Bacillota;g_Lachnospiraceae FCS020 group
– Bacillota;g_Fusicatenibacter
– Actinobacteria;g_Rothia
– Actinobacteria;g_Libanicoccus
–– Actinobacteria;g_Bifidobacterium
–– Bacillota;g_Lactobacillus
Blasto status
Negative
Positive
Age
Children
Adults
Relative abundance
31.25%
6.25%
1.25%
0.25%
0.05%
0.01%

Figure S4. Association of fecal microbiota composition with Blastocystis colonization

(A) Prevalence of *Blastocystis* detected by PCR in Amerindian villagers with low or medium urban exposure. Children were defined as ≤17 years old. The numbers of positive and total subjects are shown above each bar. *Blastocystis* prevalence was lower among children from medium–urban-exposure villages compared with those from low-exposure villages, whereas positivity was nearly universal among adults.
(B) Alpha diversity of the fecal microbiota according to *Blastocystis* status and age group. Diversity was significantly higher in *Blastocystis*-positive children, with a similar trend in adults.
(C) Differentially abundant bacterial taxa associated with *Blastocystis* status based on *16S* rRNA sequencing. Discordant taxa were identified using the ANCOM log-ratio test and are clustered by relative abundance. "+" and "–" indicate enrichment and depletion in the *Blastocystis*-positive group, respectively. Double signs "++" or "– –" indicate ANCOM $|\log_2 \text{ratio}| > 2$.

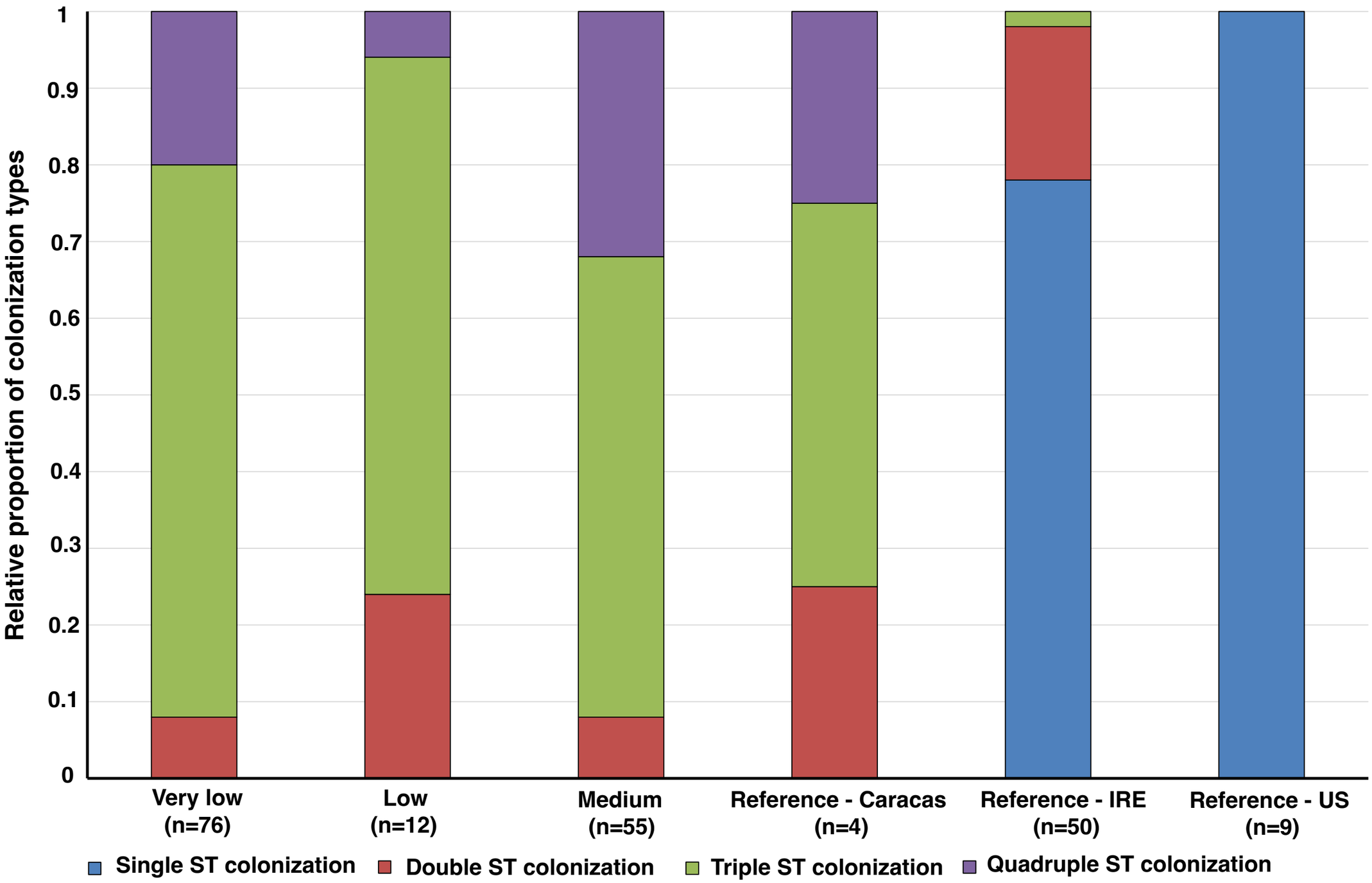

Relative proportion of colonization types
1
0.9
0.8
0.7
0.6
0.5
0.4
0.3
0.2
0.1
0
Very low (n=76)
Low (n=12)
Medium (n=55)
Reference - Caracas (n=4)
Reference - IRE (n=50)
Reference - US (n=9)
Single ST colonization
Double ST colonization
Triple ST colonization
Quadruple ST colonization

Figure S5. Distribution of Blastocystis subtype colonization patterns; related to STAR Methods

Bars show the relative frequency of single- versus multi-subtype *Blastocystis* colonization within each population group.

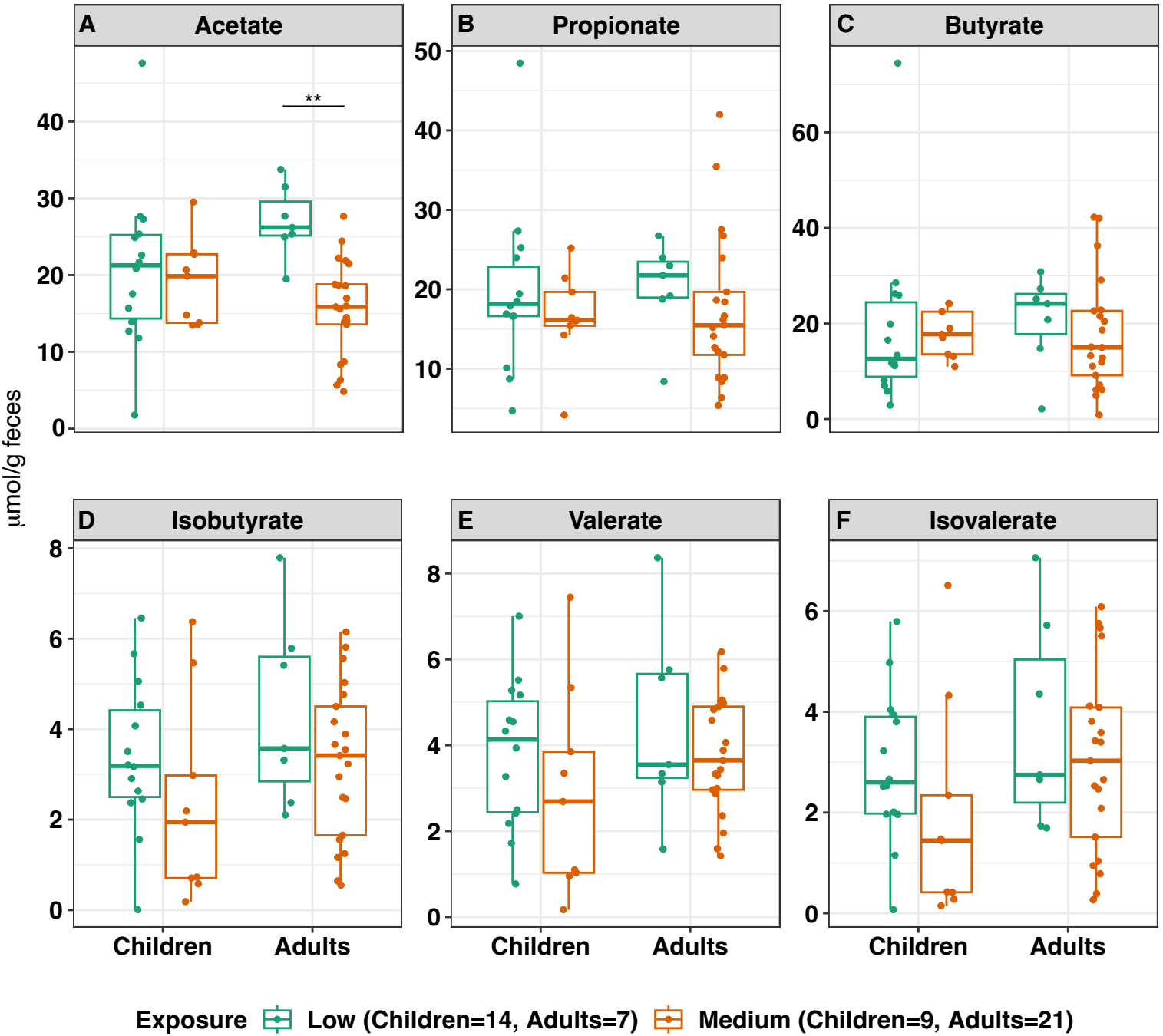

A
Acetate
B
Propionate
C
Butyrate
D
Isobutyrate
E
Valerate
F
Isovalerate
**
µmol/g feces
Children
Adults
Exposure
Low (Children=14, Adults=7)
Medium (Children=9, Adults=21)

Figure S6. Fecal short-chain fatty acid concentrations by urban exposure level; related to STAR Methods

Short-chain fatty acid concentrations measured in fecal samples collected in 2016, stratified by urban exposure level. Statistically significant differences are indicated where applicable.

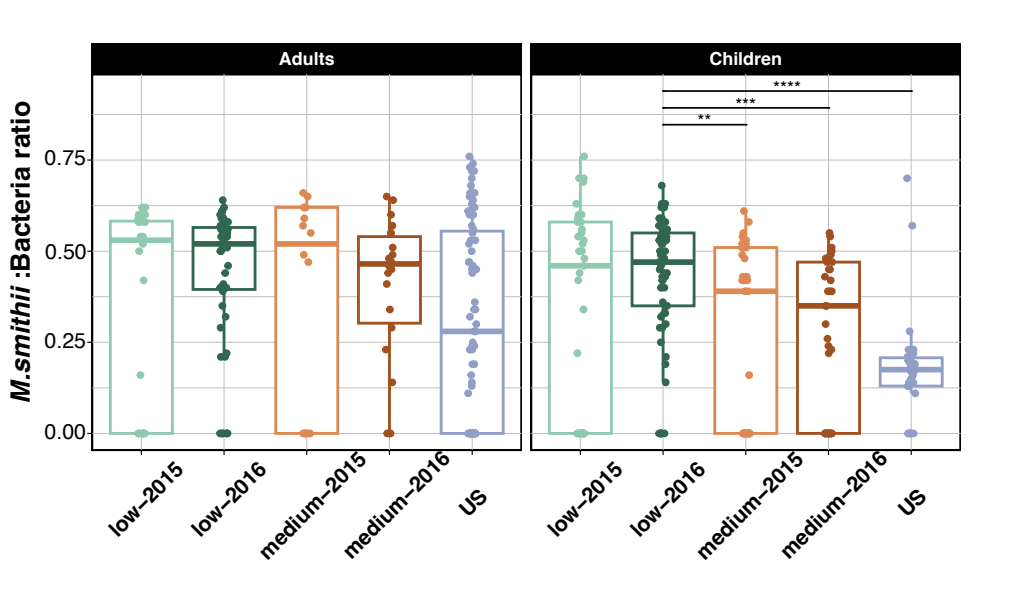

Adults
Children
M.smithii :Bacteria ratio
0.75
0.50
0.25
0.00
**
***
****
low−2015
low−2016
medium−2015
medium−2016
US

Figure S7. *Methanobrevibacter smithii* abundance across age groups and exposure levels; related to STAR Methods and Figure 2

Relative abundance of *Methanobrevibacter smithii* measured by quantitative PCR in fecal samples from children and adults collected in 2016, stratified by urban exposure level. Statistically significant differences are indicated.

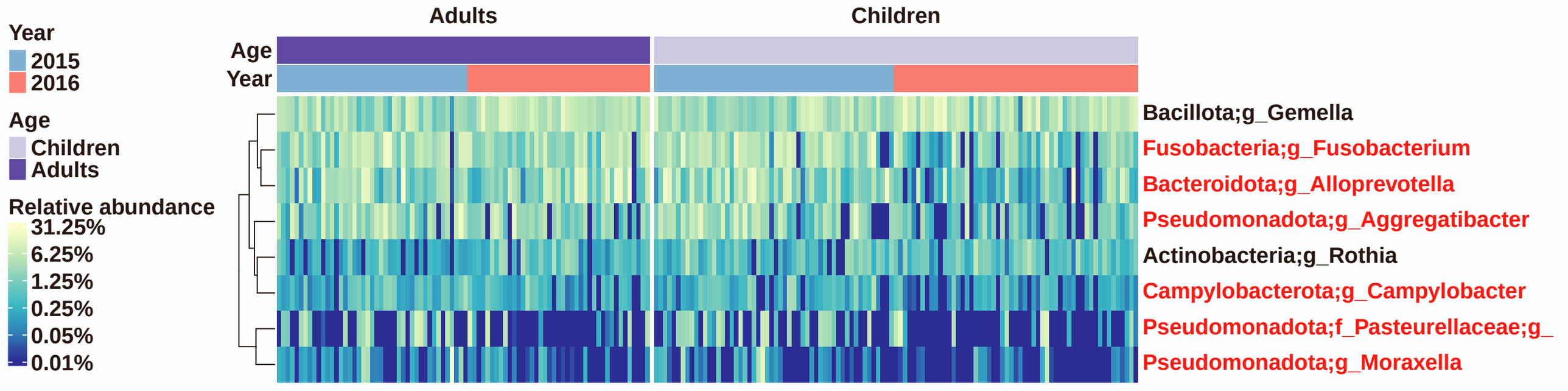

Year
2015
2016
Age
Children
Adults
Relative abundance
31.25%
6.25%
1.25%
0.25%
0.05%
0.01%
Adults
Children
Age
Year
Bacillota;g_Gemella
Fusobacteria;g_Fusobacterium
Bacteroidota;g_Alloprevotella
Pseudomonadota;g_Aggregatibacter
Actinobacteria;g_Rothia
Campylobacterota;g_Campylobacter
Pseudomonadota;f_Pasteurellaceae;g_
Pseudomonadota;g_Moraxella

Figure S8. Differentially abundant oral bacterial taxa between sampling years; related to STAR Methods and Figure 3

Differentially abundant oral bacterial taxa identified by *16S rRNA* gene sequencing between the 2015 and 2016 sampling visits in low–urban-exposure villages. Taxa shown meet the statistical significance threshold (FDR-corrected $p < 0.05$).

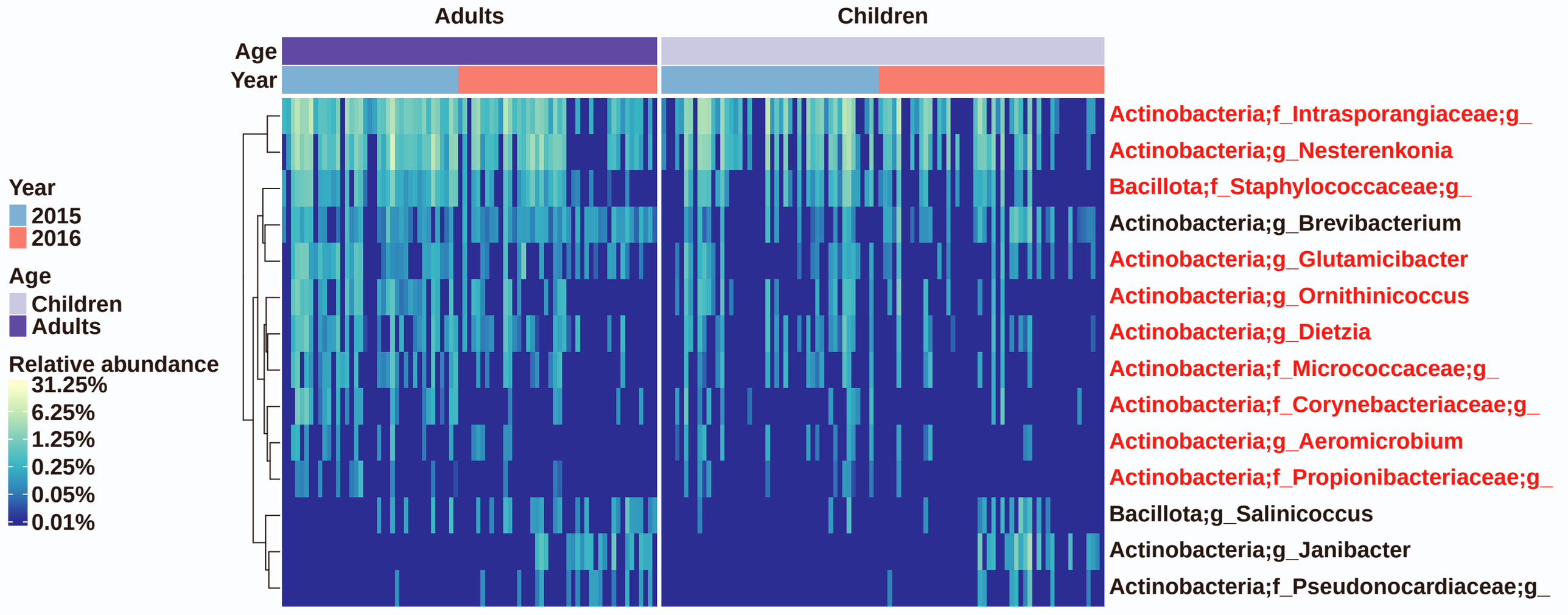

Adults
Children
Age
Year
Year
2015
2016
Age
Children
Adults
Relative abundance
31.25%
6.25%
1.25%
0.25%
0.05%
0.01%
Actinobacteria;f_Intrasporangiaceae;g_
Actinobacteria;g_Nesterenkonia
Bacillota;f_Staphylococcaceae;g_
Actinobacteria;g_Brevibacterium
Actinobacteria;g_Glutamicibacter
Actinobacteria;g_Ornithinicoccus
Actinobacteria;g_Dietzia
Actinobacteria;f_Micrococcaceae;g_
Actinobacteria;f_Corynebacteriaceae;g_
Actinobacteria;g_Aeromicrobium
Actinobacteria;f_Propionibacteriaceae;g_
Bacillota;g_Salinicoccus
Actinobacteria;g_Janibacter
Actinobacteria;f_Pseudonocardiaceae;g_

Figure S9. Differentially abundant nasal bacterial taxa between sampling years; related to STAR Methods and Figure 3

Differentially abundant nasal bacterial taxa identified by *16S rRNA* gene sequencing between the 2015 and 2016 sampling visits in low–urban-exposure villages. Taxa shown meet the statistical significance threshold (FDR-corrected $p < 0.05$).

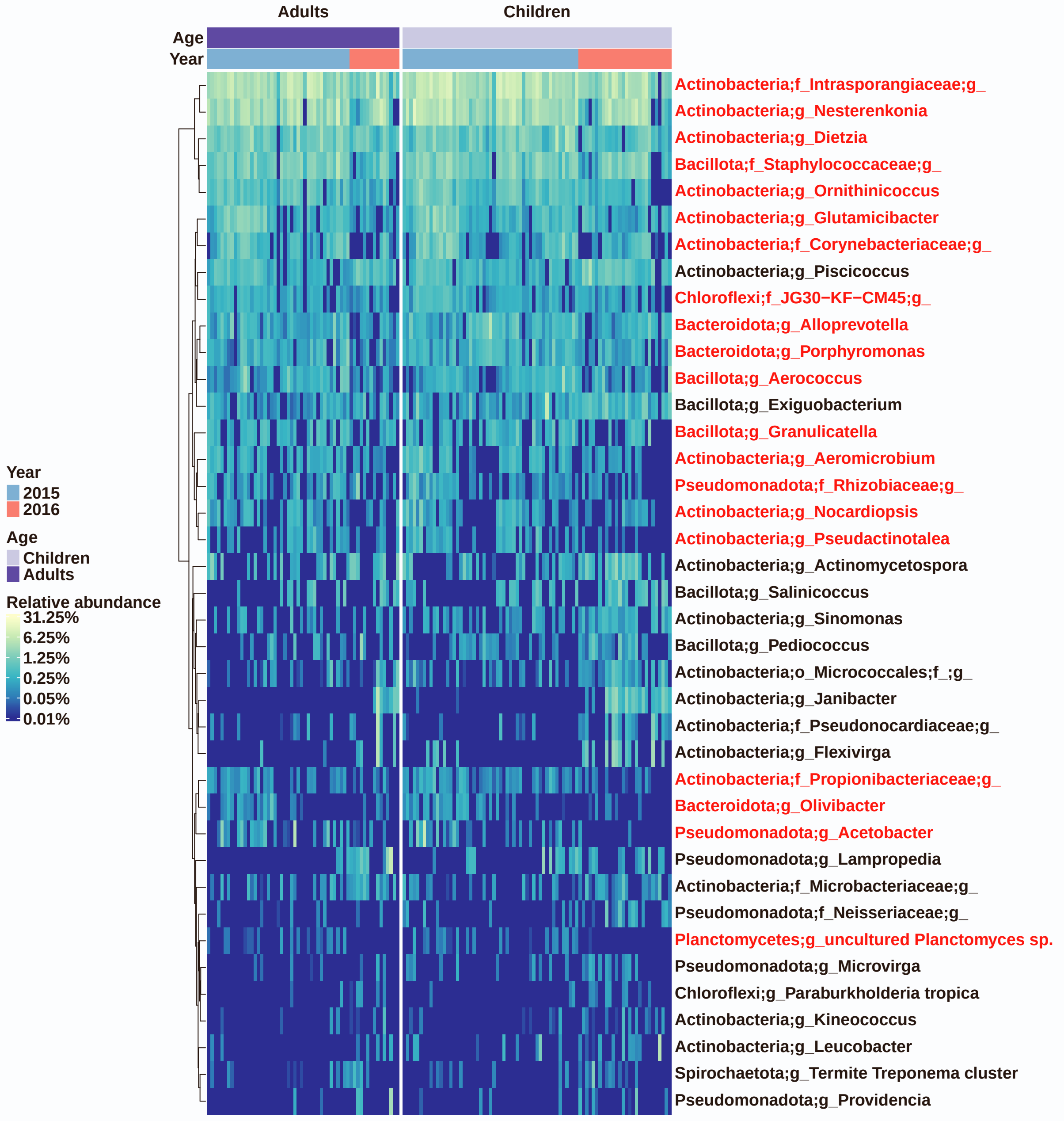

Adults
Children
Age
Year
Actinobacteria;f_Intrasporangiaceae;g_
Actinobacteria;g_Nesterenkonia
Actinobacteria;g_Dietzia
Bacillota;f_Staphylococcaceae;g_
Actinobacteria;g_Ornithinicoccus
Actinobacteria;g_Glutamicibacter
Actinobacteria;f_Corynebacteriaceae;g_
Actinobacteria;g_Piscicoccus
Chloroflexi;f_JG30−KF−CM45;g_
Bacteroidota;g_Alloprevotella
Bacteroidota;g_Porphyromonas
Bacillota;g_Aerococcus
Bacillota;g_Exiguobacterium
Bacillota;g_Granulicatella
Actinobacteria;g_Aeromicrobium
Pseudomonadota;f_Rhizobiaceae;g_
Actinobacteria;g_Nocardiopsis
Actinobacteria;g_Pseudactinotalea
Actinobacteria;g_Actinomycetospora
Bacillota;g_Salinicoccus
Actinobacteria;g_Sinomonas
Bacillota;g_Pediococcus
Actinobacteria;o_Micrococcales;f_;g_
Actinobacteria;g_Janibacter
Actinobacteria;f_Pseudonocardiaceae;g_
Actinobacteria;g_Flexivirga
Actinobacteria;f_Propionibacteriaceae;g_
Bacteroidota;g_Olivibacter
Pseudomonadota;g_Acetobacter
Pseudomonadota;g_Lampropedia
Actinobacteria;f_Microbacteriaceae;g_
Pseudomonadota;f_Neisseriaceae;g_
Planctomycetes;g_uncultured Planctomyces sp.
Pseudomonadota;g_Microvirga
Chloroflexi;g_Paraburkholderia tropica
Actinobacteria;g_Kineococcus
Actinobacteria;g_Leucobacter
Spirochaetota;g_Termite Treponema cluster
Pseudomonadota;g_Providencia
Year
2015
2016
Age
Children
Adults
Relative abundance
31.25%
6.25%
1.25%
0.25%
0.05%
0.01%

Figure S10. Differentially abundant skin bacterial taxa between sampling years; related to STAR Methods and Figure 3

Differentially abundant right arm skin bacterial taxa identified by *16S rRNA* gene sequencing between the 2015 and 2016 sampling visits in low–urban-exposure villages. Taxa shown meet the statistical significance threshold (FDR-corrected $p < 0.05$).